



Published in final edited form as:

*Matrix Biol.* 2019 May ; 78-79: 236–254. doi:10.1016/j.matbio.2018.08.008.

## Hyaluronic Acid, CD44 and RHAMM regulate myoblast behavior during embryogenesis

Yue Leng<sup>1</sup>, Ammara Abdullah<sup>2</sup>, Michael K. Wendt<sup>2</sup>, and Sarah Calve<sup>1</sup>

<sup>1</sup>Weldon School of Biomedical Engineering, Purdue University, 206 South Martin Jischke Drive, West Lafayette, IN 47907

<sup>2</sup>Medicinal Chemistry and Molecular Pharmacology, Hansen Life Sciences Research Building, Purdue University, 201 S University St, West Lafayette, IN 47907

### Abstract

Hyaluronic acid (HA) is an extracellular matrix (ECM) component that has been shown to play a significant role in regulating muscle cell behavior during repair and regeneration. For instance, ECM remodeling after muscle injury involves an upregulation in HA expression that is coupled with skeletal muscle precursor cell recruitment. However, little is known about the role of HA during skeletal muscle development. To gain insight into the way in which HA mediates embryonic myogenesis, we first determined the spatial distribution and gene expression of CD44, RHAMM and other HA related proteins in embryonic day (E)10.5 to E12.5 murine forelimbs. While HA and CD44 expression remained high, RHAMM decreased at both the protein (via immunohistochemistry) and RNA (via qPCR) levels. Next, we determined that 4-methylumbelliferone-mediated knockdown of HA synthesis inhibited the migration and proliferation of E11.5/E12.5 forelimb-derived cells. Then, the influence of CD44 and RHAMM on myoblast and connective tissue cell behavior was investigated using antibodies against these receptors. Anti-RHAMM, but not anti-CD44, significantly decreased the total distance myogenic progenitors migrated over 24 hrs, whereas both inhibited connective tissue cell migration. In contrast, anti-CD44 inhibited the proliferation of connective tissue cells and muscle progenitors, but anti-RHAMM had no effect. However, when myoblasts and connective tissue cells were depleted of CD44 and RHAMM by shRNA, motility and proliferation were significantly inhibited in both cells indicating that blocking cell surface-localized CD44 and RHAMM does not have as pronounced effect as global shRNA-mediated depletion of these receptors. These results show, for the first time, the distribution and activity of RHAMM in the context of skeletal muscle. Furthermore, our data indicate that HA, through interactions with CD44 and RHAMM, promotes myogenic progenitor migration and proliferation. Confirmation of the role of HA and its receptors

---

Corresponding Author: Prof. Sarah Calve, Tel: (765) 496-1768, Fax: (765) 494-0902, scalve@purdue.edu.

<sup>7</sup>Author contributions

Y.L. and S.C. designed the experiments. Y.L., A.A., and S.C. performed the experiments and analyzed and interpreted the data. Y.L. and S.C. wrote the manuscript. All authors critically reviewed the manuscript.

<sup>6</sup>Competing interests

The authors declare no competing interests.

**Publisher's Disclaimer:** This is a PDF file of an unedited manuscript that has been accepted for publication. As a service to our customers we are providing this early version of the manuscript. The manuscript will undergo copyediting, typesetting, and review of the resulting proof before it is published in its final citable form. Please note that during the production process errors may be discovered which could affect the content, and all legal disclaimers that apply to the journal pertain.

in directing myogenesis will be useful for the design of regenerative therapies that aim to promote the restoration of damaged or diseased muscle.

## Keywords

Hyaluronic acid; myogenesis; CD44; RHAMM; limb development; connective tissue

---

## 1. Introduction

In vertebrates, appendicular skeletal muscle is derived from the somites, which are ball-like clusters of mesodermal precursor cells that form along the anterior-posterior axis of the embryo. In the developing limb, muscle progenitors delaminate from the dorsal portion of the somite (dermomyotome) and migrate into the forelimb bud between embryonic day (E)9.5 and E10.5 [1]. These progenitor cells, or myoblasts, further differentiate into mononuclear myocytes, begin expressing myosin heavy chain isoforms and fuse into contractile, multi-nucleated myofibers [2]. A distinct population of myogenic precursor cells, called satellite cells, remain on the surface of the myofibers in a quiescent undifferentiated state [3]. The organization of these progenitors into a functional assemblage of limb muscles involves four successive phases of myogenesis [2]. Embryonic myogenesis (E10.5-E12.5; E, embryonic day) gives rise to the basic pattern. Fetal myogenesis (E14.5-birth) and neonatal myogenesis (P0-P21; P, postnatal day) are crucial for growth and maturation. Finally, adult myogenesis (P21 and later) occurs to restore functionality after injury. Each phase involves migration, proliferation, differentiation, and fusion of myogenic precursors into multinucleate myofibers. A number of biochemical and mechanical factors are important regulators during myogenesis. In particular, it has been demonstrated that the surrounding connective tissue directs the organization of muscle in the developing limb [4,5]. The connective tissue is primarily comprised of fibroblasts and the extracellular matrix (ECM) these cells secrete [4,5]; however, the exact composition of the ECM and how it directly regulates embryonic myogenesis remains unknown.[76,80,88,89]

ECM in adult skeletal muscle can be classified into two layers: a basement membrane that surrounds individual myofibers and an interstitial matrix that fills the intercellular spaces [6]. The basement membrane is comprised of a basal lamina, primarily made up of type IV collagen and laminin, and a type VI collagen-containing fibrillar reticular lamina that links the basal lamina to the interstitial matrix [7,8]. The interstitial matrix consists of fibrillar collagens, elastin, proteoglycans, fibronectin, and hyaluronic acid (HA) [6,9,10]. During muscle repair and regeneration, the ECM undergoes significant remodeling. There is a transient upregulation of tenascin-C, fibronectin, and HA, which have been shown to facilitate the scar-free restoration of the musculature [9,11]. It is likely that similar ECM remodeling occurs during muscle development as it has been shown that HA is highly expressed in the developing limb and participates in various aspects of morphogenesis [12–14]. During the early stages of limb bud outgrowth, HA is prominent at sites where cell migration occurs [15], and enhances mesenchymal cell migration and division [12,16]. Moreover, conditional inactivation of HAS2 within the limb mesoderm revealed an important role for HA in regulating skeletal growth, patterning, chondrocyte maturation, and

joint formation in developing limbs [14]; however, the effect of HA on the behavior of myogenic progenitors is unclear.

HA is a negatively charged, linear glycosaminoglycan that is found throughout the ECM of all vertebrate tissues, on the cell surface, and even inside cells [17]. Individual HA molecules are typically made up of 2,000 to 25,000 disaccharides, with a high molecular weight of  $10^6$ - $10^7$  Da and extended molecular lengths of 2 to 25 $\mu$ m [18]. These characteristics help regulate the hydration and viscosity of HA-containing tissues and contribute directly to the remodeling and cellular events that drive embryonic morphogenesis, tissue regeneration, and tumorigenesis [19,20]. Through interactions with HA-binding proteoglycans (*e.g.* aggrecan and versican), HA maintains extracellular and pericellular matrix structural integrity via provision of a hydrated zone which facilitates cellular invasion during development and tissue remodeling [17,21].

In addition, HA acts as a signaling molecule and mediates cellular behavior by binding to cell surface receptors, including the cluster of differentiation 44 (CD44) [22] and the receptor for HA-mediated motility (RHAMM) [23,24]. CD44 is an ubiquitous, multi-domain cell surface glycoprotein that is considered to be the principal HA receptor [22]. The N-terminal extracellular “link module” directly binds to HA. The C-terminal cytoplasmic tail is important for CD44-mediated intracellular signal transduction [25,26]. Cell type, cytoplasmic tail phosphorylation and receptor clustering affect the activation state of CD44 and subsequently binding with HA [27]. HA-CD44 binding influences diverse processes, including cell-cell and cell-matrix adhesion, cell migration during development, inflammation, tumor growth, and metastasis [28,29]. In particular, the interaction between HA and CD44 is required for early adhesive cell-cell interactions of limb bud mesenchyme during limb bud outgrowth [30]. CD44 also regulates growth and tissue integrity by mediating the cellular uptake and degradation of HA [31,32].

RHAMM (also known as CD168) [24], an acidic, coiled-coil protein expressed by many cell types, localizes to the nucleus, cytoplasm, and cell surface [33]. It is thought that RHAMM binds HA via a BX7B motif on the -COOH terminus [21,34]. Nuclear RHAMM, when bound to extracellular signal-regulated kinase 1/2 (ERK1/2) and mitogen-activated protein kinase (MEK), participates in cell motility and inflammation [35]. Cytoplasmic RHAMM interacts with microtubules and actin filaments in the cytoskeleton either directly, or through binding with microtubule- and centrosome-related proteins, to affect cell polarity and direct cell migration [35–37]. Extracellular RHAMM influences cellular transformation and cell migration during tissue injury and repair in a HA-dependent manner [23]. In addition, RHAMM interacts with CD44, HA, and growth factors to activate protein tyrosine kinase signaling cascades that activate the ERK1,2 -MAP kinase cascade, which increases random motility [35].

Although RHAMM and CD44 can participate independently in regulating cellular behaviors, their relative contributions are not clearly understood. When knocked out *in vivo*, these receptors have redundant or overlapping functions that can compensate for each other as evidenced by the viability of CD44-knockout and RHAMM-knockout mice [38–40]. For example, in a collagen-induced arthritis model, the development of arthritis depended on

CD44 in wild-type mice. However, in CD44-knockout mice, RHAMM expression was upregulated to compensate for the loss of CD44 and the induction of arthritis was RHAMM-dependent [39]. Muscle repair is also influenced by CD44, wherein CD44- knockout mice show delayed repair in a tibialis anterior injury model [41]. Subsequent *in vitro* studies with myoblasts isolated from these mice indicated that lack of CD44 negatively influenced cell migration and differentiation [41]. Although many studies have shown RHAMM binds to HA to mediate cell migration [42,43], to date there have been no investigations into the role of RHAMM in skeletal muscle. Moreover, the relative contribution of the two types of HA receptors and the intracellular signaling pathways involved in HA-mediated effects in myogenesis remain unknown.

To investigate the role of HA, RHAMM and CD44 in myogenesis, we used the mouse forelimb as a model system. We hypothesized that HA instructs myogenic progenitor cell migration and proliferation by interacting with the receptors RHAMM and CD44. First, the distribution of all three molecules was visualized in the context of embryonic myogenesis *in vivo* using Pax3-Cre/ZsGreen1+ mice in which myogenic progenitors are GFP+. The gene expression of HA, RHAMM, and CD44, as well as the hyaluronic acid synthases (HAS1 – 3) and hyaluronidases (HYAL1 – 4), were compared between GFP+ myoblasts and the surrounding GFP- connective tissue cells. Then, the influence of endogenous HA on myoblast proliferation and migration was investigated *in vitro* using the HA polymerization inhibitor 4- methylumbelliferone (4MU). Antibodies against CD44 and RHAMM were used to specifically block the interaction of HA with these receptors to determine the role of each on myogenesis. Finally, CD44 and RHAMM were depleted using shRNA to further confirm their function. We found that CD44 and RHAMM have functional overlap in modulating cell behaviors and both receptors regulate motility and proliferation of myoblasts and connective tissue cells.

## 2. Results

### 2.1. The distribution of CD44, RHAMM and HA spatially and temporally vary during forelimb development.

Although HA is known to influence myogenesis [44], the expression, distribution, and function of HA and its receptors CD44 and RHAMM during muscle development have not been fully characterized. To gain preliminary insight into the role that HA and its receptors play in myogenesis, a spatiotemporal map of these components in E10.5-E12.5 murine embryos was generated. Myogenic progenitors were labeled with GFP using embryos heterozygous for Pax3-Cre and ROSA-ZsGreen. Pax3 expression in the limb bud is largely restricted to myogenic progenitors; however, it has also been found in a small subset of endothelial cells that contribute to the vasculature of the limb [45]. These Pax3+ endothelial cells make up a small fraction of the limb vasculature and are predominantly found in the vessels below the epidermis [45]. Therefore, the majority of the GFP+ cells within the limb can be considered to be myoblasts.

HA, CD44, and RHAMM were widely distributed throughout the developing limb (Fig. 1). Mononucleated GFP+ myoblasts migrated from the somites into the early forelimb bud by E10.5, separated into distinct dorsal and ventral muscle masses by E11.5 and started to

elongate by E12.5 (Fig. 1A, F, K). CD44 was evenly distributed in the forelimb at E10.5 and E11.5 (Fig. 1B, G); however, at E12.5, CD44 aggregated around the dorsal (denoted as “d”) and ventral (denoted as “v”) muscle masses (Fig 1L). RHAMM co-localized with the GFP+ muscle progenitor cells at all stages, but the expression decreased from E10.5 - E12.5 (Fig. 1C, H, M). HA was broadly distributed throughout the limb and around the myoblasts (Fig. 1D, I, N). Interestingly, HA expression was lower in dorsal and ventral muscle masses at E12.5, whereas HA was significantly upregulated around the newly forming joints and the distal tip of the limb (Fig 1N). At higher magnifications, CD44 and RHAMM appeared to colocalize with HA (Fig. 1P, R, S, U, Y, X) and the surface of GFP+ muscle cells (Fig. 1Q, T, W). At E12.5, in areas where myoblasts began taking on a more elongated phenotype, CD44 and RHAMM expression decreased (Fig 1W).

To determine how muscle progenitors and the surrounding connective tissue cells differentially bind to, and regulate the metabolism of, HA during development, gene expression was analyzed using quantitative PCR. Cells from Pax3-Cre/ZsGreen+ E10.5-E12.5 forelimbs were separated into GFP+ and GFP- populations using FACS. Since the connective tissue in the embryo forelimb at these stages is primarily composed of fibroblasts [5], we consider the GFP+ cells to be predominantly muscle progenitors and the GFP- cells to be predominantly fibroblasts. Target gene expression was normalized to the housekeeping gene *β-actin*. *CD44* was broadly expressed in both cell populations with ACq in the magnitude of  $10^{-1}$  (Supplemental Fig. 1). Two-way ANOVA revealed that developmental stage (E10.5/E11.5/E12.5;  $p=0.001$ ) and the interaction between stage and cell type ( $p<0.05$ ) significantly affected *CD44* expression.

The expression of the three HA synthases *HAS1-HAS3* and four hyaluronidases, *Hyal1-Hyal4*, were measured to evaluate how HA deposition was regulated in the developing forelimb. *HAS1* expression in GFP+ cells was significantly influenced by stage (shown by two-way ANOVA,  $p<0.01$ ; Fig 2C). *HAS2* in GFP+ cells was upregulated at E12.5 (Fig 2D). GFP- cells expressed significantly more *HAS3* than GFP+ cells (shown by two-way ANOVA,  $p<0.001$ ; Fig 2E). The overall expression of *HAS2* was greater than the other synthases (Supplemental Fig. 1), which is consistent with previous reports describing it to be the predominant HAS during development [46]. *Hyal2* was the dominant hyaluronidase expressed in murine forelimb; however, the expression of *Hyal1*, *Hyal2*, *Hyal3*, and *Hyal4* showed no significant difference as a function of developmental stage in either cell population (Fig. 2, Supplemental Fig. 1).

## 2.2. 4MU reduces HA deposition and inhibits migration of embryonic forelimb cells

To investigate the role of endogenous HA in regulating muscle cell migration, we used 4-methylumbelliferone (4MU), an inhibitor of HA biosynthesis [47]. 4MU decreases HA deposition by depleting UDP-glucuronic acid (UDP-GlcUA), one of the saccharide precursors for HA, and inhibits the transcription of *HAS1 - HAS3* [48]. Primary mesenchymal cells, comprising a heterogeneous population of GFP+ and GFP- cells, were isolated from E10.5/E11.5 Pax3-Cre/ZsGreen+ forelimbs, cultured *in vitro* with 0 – 1.0 mM 4MU, and imaged every hour for 24 hrs using time-lapse microscopy. Three types of culture media (DMEM, DMEM+10%FBS, and adv DMEM, see 4.4 for details) were used to

exclude the effect of serum on migration. There was no apparent difference in cellular viability or morphology of GFP+ cells incubated in the absence or presence of FBS. For all three media, GFP+ cells co-cultured with 0.5mM 4MU and 1.0mM 4MU migrated significantly slower than the control ( $p < 0.0001$ ; Fig 3A). One way ANOVA indicated that adding 4MU in all three culture medium significantly influenced GFP+ cells migration ( $p < 0.0001$ ). The inhibitory influence of 4MU on HA synthesis was confirmed by labeling with biotinylated hyaluronic acid binding protein (HABP) and indicated that 4MU reduced the deposition of HA in a dosage-dependent manner (Fig 3B).

### 2.3. Anti-RHAMM but not anti-CD44 inhibits myogenic progenitor migration

To investigate the involvement of two of the predominant HA receptors, CD44 and RHAMM, in controlling cell migration, the *in vitro* expression of these proteins and the effects of antibodies against CD44 and RHAMM on primary myoblast migration were studied. GFP+ and GFP- cells were isolated using FACS to rule out the influence of reciprocal signaling between the two populations on migration. Cells were cultured in growth medium for at least 16 hrs before adding antibodies to promote the deposition of HA. Then, we performed time-lapse imaging for cells in the presence of IgG control, anti-CD44, anti-RHAMM, or anti-CD44 + anti-RHAMM (all antibody concentrations = 100  $\mu$ g/ml). Anti-RHAMM and anti-CD44 + anti-RHAMM significantly inhibited GFP+ cell motility ( $p < 0.0001$ ) whereas there was no difference between control and anti-CD44 treated cells (Fig. 4A). In contrast, both anti-CD44 and anti-RHAMM significantly decreased GFP- cell motility, but no additive effect was observed ( $p < 0.0001$ ; Fig. 4B). Two-way ANOVA showed that antibody treatment, cell type and their interaction had a significant impact on cell migration ( $p < 0.0001$ ). The same trends were observed in unsorted cell populations (Supplemental Fig. 2). After the initial antibody treatment, a heterogeneous population of cells was treated again with primary antibodies and then stained with secondary labeling reagents to confirm there was no binding of the IgG control and to visualize the distribution of CD44 and RHAMM after 24 hour antibody treatment. CD44 localized to the membrane in the majority of cells (Fig. 4C, E, F, H); however, the distribution and cellular localization of RHAMM was more variable (Fig. 4C), consistent with previous descriptions that RHAMM localizes to the nuclear, cytosolic, membrane-bound and extracellular compartments [33,49]. Both receptors co-localized with HA (Fig. 4D, E, G, H). Interestingly, the expression of RHAMM appeared to increase after treatment with anti-RHAMM and anti-CD44 + anti-RHAMM (Fig. 4F, G).

### 2.4. The transcription of HA-related genes changes after antibody treatment

RHAMM protein expression appeared to increase after treating cells with anti-RHAMM (Fig. 4F, G). Thus, we performed qPCR to assess how HA-related genes were affected by treatment with antibodies for 24 hrs (Fig. 5, Supplemental Fig. 3). Since *HYAL3* and *HYAL4* were expressed at low levels in the forelimb (Fig. 2, Supplemental Fig. 1), we did not include these two genes in this investigation.

For GFP+ cells, incubation with anti-RHAMM and anti-CD44 + anti-RHAMM promoted more *RHAMM* compared to IgG control (Fig. 5), consistent with the immunohistochemical results (Fig. 4). One-way ANOVA revealed that adding antibodies significantly influenced



*RHAMM* expression in GFP<sup>-</sup> cells ( $p < 0.05$ ). Moreover, we found *CD44* and *HAS2* expression increased with anti-RHAMM and anti-CD44 + anti-RHAMM treatment. Cells upregulated the expression of *HYAL2* in response to anti-CD44 + anti-RHAMM compared with IgGs control (Supplemental Fig. 3). Consistent with the GFP<sup>+</sup> population, GFP<sup>-</sup> cells expressed more *RHAMM* after incubation with anti-RHAMM and anti-RHAMM + anti-CD44. However, GFP<sup>-</sup> cells were less affected by antibody treatment when compared to GFP<sup>+</sup> cells. *HYAL1* expression was downregulated in anti-CD44 + anti-RHAMM treated cells compared to anti-CD44 (Supplemental Fig. 3).

## 2.5. 4MU inhibits proliferation of embryonic forelimb cells

In addition to migration, proliferation is crucial for establishing the musculature in the developing forelimb. To examine the role of HA in supporting cell proliferation, a heterogeneous population of GFP<sup>+</sup> and GFP<sup>-</sup> cells isolated from E10.5/E11.5 forelimbs were cultured *in vitro* with 0mM - 1.0mM 4MU for 24 hrs. During this period of time, cells were also incubated with 5 $\mu$ M EdU to identify cells that have reentered the cell cycle [50]. 4MU significantly decreased EdU incorporation by both GFP<sup>+</sup> and GFP<sup>-</sup> cells in a dose-dependent manner (Fig. 6). Two-way ANOVA revealed the proliferation rate of GFP<sup>+</sup> and GFP<sup>-</sup> cells were significantly affected by 4MU ( $p < 0.001$ ), wherein cell cycle re-entry was affected more in GFP<sup>+</sup> cells than GFP<sup>-</sup> cells ( $p < 0.0001$ ).

## 2.6. Anti-CD44 but not anti-RHAMM inhibits myogenic progenitor proliferation

To examine if CD44 and RHAMM play a role in regulating cell proliferation *in vitro*, GFP<sup>+</sup> and GFP<sup>-</sup> cells isolated using FACS were incubated with 5  $\mu$ M EdU in combination with anti-CD44, anti-RHAMM, both antibodies or isotype controls for 24 hrs. Antibody treatment significantly affected the proliferation of GFP<sup>+</sup> cells (one-way ANOVA,  $p < 0.05$ ). For GFP<sup>+</sup> cells, anti-CD44 but not anti-RHAMM inhibited proliferation ( $p < 0.05$ , Fig. 7). Interestingly, cells incubated in anti-CD44 + anti-RHAMM did not significantly inhibit DNA synthesis.

## 2.7. ERK1,2 phosphorylation in GFP<sup>+</sup> myoblasts are affected by anti-CD44 and anti-RHAMM

To determine whether antibody treatment affected ERK1,2 phosphorylation in GFP<sup>+</sup> cells, a known downstream effect of HA binding [29,43,51], we quantified serum induction of ERK1,2 activity using an ELISA. After stimulation with 10% FBS, ERK1,2 was activated in all the groups, but activity was significantly less in antibody treated cells (one-way ANOVA,  $p < 0.001$ ; Fig. 8). Moreover, there was an additive effect when anti-CD44 and anti-RHAMM were combined. The difference in ERK1,2 activity between groups was not due to a decrease in total ERK1,2 protein levels because the cells in all four groups expressed similar amounts of ERK1,2 protein (data not shown). These results suggest that the activation of CD44 and RHAMM is required for sustaining ERK1,2 activity in culture.

## 2.8. shRNA-mediated depletion of CD44 and RHAMM inhibit myogenic progenitor migration and proliferation

Inhibition of CD44 and RHAMM using antibodies led to differential decreases in migration in proliferation, which contrasted with our 4MU results that showed knockdown of HA synthesis affected these cellular behaviors in both cell types. Antibody-blocking experiments may not fully inhibit receptor signaling as it primarily affects receptors located on the cell surface and may not be able to engage all isoforms or receptors within complexes. Therefore, GFP+ and GFP- cells isolated using FACS were transduced with lentiviral particles encoding shRNAs targeting CD44, RHAMM, or a nontargeting, scrambled shRNA as a control. Depletion of CD44 and RHAMM in both cells was verified using immunoblot (Fig. 9A) and qRT-PCR (data not shown). In response to transduction with shCD44 or shRHAMM, both GFP+ and GFP- cells showed a significant decrease in total distance traveled and proliferation rate. For both types of cells, the decrease in cell migration was comparable to that observed after treatment with 4MU (Fig. 3), whereas the inhibition in proliferation was more pronounced after shRNA-mediated depletion of CD44 and RHAMM compared to that observed after treatment with 4MU (Fig. 6) and incubation with antibodies (Fig. 7).

Taken together, our data indicate HA and its receptors, CD44 and RHAMM, play significant roles in mediating myogenic and connective tissue cell migration and proliferation during development.

## 3. Discussion

The binding between HA and its receptors, CD44 and RHAMM, has been shown to control many types of cellular behavior [51–54]; however, the direct effect of these molecules on myoblast migration and proliferation during muscle development had not been previously investigated. Using a mouse model in which myoblasts are GFP+ and the remaining forelimb cells are GFP-, our study demonstrates that HA, CD44 and RHAMM play functional roles in embryonic myogenesis. Immunohistochemistry revealed that HA was widely expressed in the developing forelimb and myoblasts and the surrounding connective tissue cells expressed CD44 and RHAMM. Knockdown of HA *in vitro* using 4MU, and CD44 and RHAMM via shRNA, significantly inhibited the migration and proliferation of both cell types. In contrast, antibody blocking of CD44 and RHAMM induced differential effects on cell behavior, indicating that these receptors may be associated with different complexes depending on cell type. Collectively, our data show that cells within the limb utilize both CD44 and RHAMM to interact with HA during development.

This is the first study documenting both the expression dynamics and functional roles of CD44 and RHAMM in developing forelimb cells. Around E10.5, when muscle progenitors delaminate from the somite and migrate into the forelimb bud, RHAMM is highly expressed (Figs. 1, 2). By E12.5, the expression of RHAMM is significantly downregulated (Figs. 1, 2). At E12.5 myoblasts have begun to establish the basic pattern of the musculature and take on a more differentiated phenotype [55]. Our immunohistochemical and gene expression data, in combination with time-lapse imaging demonstrating that anti-RHAMM inhibits myoblast migration (Fig. 4), supports this view and indicates that RHAMM is



downregulated once the cells have reached the appropriate place within the limb to prevent further migration. A similar downregulation of RHAMM was correlated with osteoblastic cell differentiation [56].

Our data indicate that HA promotes myoblast proliferation (Fig. 6), which may be mediated by the ability of HA regulate cell shape during the G1, S, and G2 phases [12]. In addition, this may be due to CD44 and RHAMM signaling as we found that anti-CD44, shCD44 and shRHAMM affected myoblast proliferation (Fig. 7, 9C). Our results contrast with a previous study showing that myoblasts from CD44-knockout mice show no difference in proliferation compared with wild-type cells [41]. The disparity is likely due to differences in experimental protocols, as they labeled wild-type and CD44-knockout myoblasts with BrdU for only 1 hr [41], whereas we incubated cells with EdU for 24 hrs. Additionally, the expression of other HA receptors likely increased in CD44-knockout cells to compensate. This type of compensation may also explain why lung fibroblasts from CD44-knockout mice also showed no difference in motility, whereas our results showed that anti-CD44 significantly decreased the migration of GFP- cells (Fig. 4). Surprisingly, cells treated with both anti-CD44 + anti-RHAMM did not show any difference in proliferation. We hypothesize that the addition of anti-RHAMM could affect the affinity of CD44 binding to the antibody, since CD44 and RHAMM are known to form complexes on the cell surface [29].

Based on our findings that both CD44 and RHAMM have significant impacts on embryonic myoblast behavior, whether mice deficient in CD44 or RHAMM have abnormal limb formation needs to be considered. During development, CD44<sup>-/-</sup> mice are viable with normal growth and appearance [38,57,58], which may be contributed to compensation by other molecules. However, an antibody-blocking experiment that interfered with CD44 variants CD44v3 and CD44v6 disrupted limb outgrowth in rat embryos cultured in vitro [58]. In that system, compensation for CD44 deficiency may no longer be possible when induced at later stages of development. RHAMM knockout mice are also viable without obvious deficiencies [40], even though RHAMM has been described to be essential for a variety of several cellular events that are required for tissue formation such as cell migration, proliferation, and ECM remodeling [35]. Surprisingly, RHAMM-CD44 double-knockout mice did not develop any significant abnormalities, suggesting that there might be other HA receptors or molecules redundant with and compensate for RHAMM and CD44 [20,43].

Our data are the first findings that describe changes in *HAS* and *Hyal* gene expression in skeletal muscle during forelimb development and indicate that myoblasts and the surrounding cells are capable of regulating the deposition of HA (Fig. 2). *HAS2* mRNA was expressed at higher levels compared to other isoforms (Supplemental Fig. 1), and increased by 2-fold from E10.5 to E12.5 in both cells (Fig. 2). Multiple studies have shown that *HAS2* plays a predominant role in inducible HA synthesis in muscle cells [11] and fibroblasts [59–61]. *HAS1* expression level was the lowest (Supplemental Fig. 1), and did not significantly vary over myogenesis. This corresponds to a previous study which showed *HAS1* is primarily found during gastrulation (E7.5-E8.5) [62] and it maintains a basal level of HA synthesis during embryogenesis whereas *HAS2* encourages cell migration and invasion [63]. Significantly more *HAS3* mRNA was expressed by GFP- cells compared to GFP+ cells (Fig. 2, Supplemental Fig. 1), which suggests a preferential synthesis of low molecular weight HA

in GFP- since HAS3 produces HA chains less than  $10^6$  Da [64]. The developing vasculature was likely the source of *HAS3* as our previous study showed HAS3 was localized to the vessels in adult muscle [11]. Hyals are involved in tissue remodeling during development, of which Hyal1 and Hyal2 are the two most abundant and important [65]. Our results showed increased expression of Hyal1- Hyal 4 suggesting catabolism of high molecular weight HA is a feature of forelimb development. By breaking down HA, the interstitial barrier was hydrolyzed, tissue permeability was thereby increased [66]. The overall increase of HAS2 and HAS3, concomitant with upregulated Hyal1- Hyal4, indicates rapid ECM remodeling tissue during myogenesis.

We used 4MU to investigate how knockdown of HA influenced the migration and proliferation of embryonic muscle precursors. Though commonly described as a specific inhibitor of HA synthesis by depleting the HA precursor UDP-GlcUA [48], 4MU has also been reported to affect the regulation of UDP-glucose dehydrogenase (UGDH), a key enzyme required for both HA and sulfated- glycosaminoglycan production [67]. In addition, 4MU has been shown to downregulate the expression of CD44, RHAMM [68], and downstream effectors in the HA signaling cascade such as phospho-ErbB2, phospho-Akt, matrix metalloproteinases 2 and 9 [69,70]. However, our results viewed collectively indicate that the effect of 4MU on embryonic forelimb cell proliferation and migration *in vitro* is linked to the knockdown of HA synthesis (Figs 3, 6). Through histology, we confirmed that 4MU substantially reduced HABP reactivity (Fig. 3) and perturbation of cell - HA interactions via incubation with anti- CD44 and anti-RHAMM significantly affected cell migration and proliferation (Figs 4, 7).

After antibody treatment, we investigated how the expression of CD44, RHAMM and other HA- associated molecules changed. Immunohistochemistry revealed a higher level of RHAMM after treatment with anti-CD44 and anti-RHAMM compared with control (Fig. 4). Quantitatively, *RHAMM* expression significantly increased in anti-RHAMM, and anti-RHAMM + anti-CD44 treated groups (Fig. 5). Similar observations of RHAMM compensation have been documented in CD44-knockout mouse models [39,71]. The overall increase in expression of both receptors in response to antibody treatment highlights the importance of RHAMM and CD44, and HA-specific signaling for cells.

Moreover, we showed that interfering with CD44 and RHAMM affects ERK signaling. CD44 and RHAMM are thought to play roles in controlling extracellular signal-regulated kinase (ERK), which has a significant role in HA-mediated cell motility and cellular proliferation [43,72]. ERK1,2 acts downstream of cell surface CD44 and RHAMM in these pathways [43,73]. As expected, treatment of GFP+ cells with antibodies against CD44 and RHAMM led to attenuated activation of ERK1,2 in culture. Addition of both antibodies in combination exhibited a more inhibitory effect on ERK1,2 activation. These results together showed that HA-CD44 and HA-RHAMM interactions are crucial in regulating myoblast behavior during forelimb development.

ShRNA depletion confirmed that both CD44 and RHAMM are important mediators of HA signaling in myogenic and connective tissue cell migration and proliferation. Similar to cells treated with 4MU (Fig. 3), migration was inhibited in CD44- and RHAMM-depleted cells

compared to the controls (Fig. 9), whereas no significant effect was found in anti-CD44 treated GFP+ cells (Fig. 4). The differential results between the antibody and shRNA depletion studies can mainly be explained by the limitation of the anti-CD44 we used. First, the antibody detects a standard 85kDa isoform of CD44 [74]; whereas there are many CD44 isoforms [29,75]. Second, anti-CD44 binds to the “link” domain on cell surface CD44. The “link” domain enables CD44 to bind to HA [26]; however, the affinity or the percentage of binding may not be that strong. Third, the blocking effect of the antibody against CD44 may act for less than 24 hours. The variability of effectiveness using CD44 blocking antibodies between experiments has also been described [20]. These three reasons indicate the antibody may not fully interrupt the interaction between HA and CD44. In addition, HA is the principal, but by no means the only, ligand of CD44. Other ECM components can bind to CD44, including type I and type VI collagen [77,78], fibronectin [79], laminin, and chondroitin sulfate [81]. The antibody may not be able to interfere with the interaction between CD44 and these ligands. In contrast, shCD44 depletion impeded any CD44-binding ligands from influencing GFP+ cell migration.

For proliferation, the inhibitory effects of CD44 and RHAMM depletion were clear, *i.e.* there was about 80% reduction in the number of EdU+ cells (Fig. 9). Cells treated with 0.5mM and 1.0mM 4MU also showed a remarkable decrease in DNA synthesis, but to a lesser degree than those transfected with shCD44 and shRHAMM. Due to the limited solubility of 4MU in growth medium, we were unable to increase the concentration of 4MU to have a similar effect. While CD44 antibody treatment decreased proliferation rate, it was less pronounced than in shCD44 and shRHAMM transfected cells. Again, since the blocking effectiveness using antibodies may not be complete, it is reasonable to have stronger inhibition results with shRNA-mediated depletion. The difference in proliferation between anti-RHAMM and shRHAMM may be attributed to the different function of cell surface RHAMM and intracellular RHAMM [33]. Intracellular RHAMM, a mitotic spindle protein, has been shown to control mitotic spindle stability, and thus affecting cell proliferation. However, anti-RHAMM binding to surface RHAMM, may not affect the DNA synthesis of cells. Although a previous study reported that antibody blocking of cell surface RHAMM signaling resulted in anti-proliferative effect of fibrosarcoma cells through the G2/M DNA damage checkpoint [82], the varied role of surface RHAMM may be attributed to differences in antibody, antibody efficiency, as well as other differences including cell type, HA origin and molecular weight. The different mechanisms behind how antibody and shRNA treatments affect cells may also explain other studies in which the differential effect of anti-RHAMM and anti-CD44 has been documented; RHAMM, but not CD44 was required for HA-mediated arterial smooth muscle cell [42], endothelial cell [83], and B cell [84] motility.

Our study established that CD44 and RHAMM activation promote myogenic and connective tissue migration and proliferation. These findings are in agreement with previous reports suggesting that CD44 and RHAMM have some overlapping functions in regulating cell behavior when interacting with HA [39,85]. The discrepancies between our antibody blocking and shRNA depletion studies indicate that many details regarding HA-receptor mediation of cell migration and proliferation remain to be characterized. For example, RHAMM is not an integral membrane protein and must cooperate with other receptors to compensate when CD44 activity is inhibited in order for HA-specific signals to be

transmitted from the outside to the inside of the cell. However, the identities of these additional proteins have not yet been documented. Therefore, our future challenge is to further investigate how HA regulates cellular activities to gain a deeper understanding into how HA directs myogenesis.

## 4. Materials and Methods

Unless otherwise specified, all reagents were of cell culture grade from Sigma-Aldrich.

### 4.1. Tissue acquisition

All murine experiments were approved by the Purdue Animal Care and Use Committee (PACUC; protocol #1209000723). PACUC ensures that all animal programs, procedures, and facilities at Purdue University adhere to the policies, recommendations, guidelines, and regulations of the USDA and the United States Public Health Service in accordance with the Animal Welfare Act and Purdue's Animal Welfare Assurance. Pax3-Cre [86] and ROSA-ZsGreen1 transgenic mice [87] were obtained from the Jackson Laboratory (Bar Harbor, ME, USA) and used to generate Pax3-Cre/ZsGreen1+ embryos in which all Pax3-expressing cells and their progeny are GFP+. Within the forelimb, the majority of GFP+ cells are of the skeletal muscle lineage (>90%), whereas the remainder are endothelial cells [45]. Males heterozygous for the Pax3-Cre transgene were time-mated with females homozygous for ROSA-ZsGreen1 and noon on the day a copulation plug was found was designated as embryonic day (E)0.5. E10.5-E12.5 Pax3-Cre/ZsGreen1+ embryos were harvested from dams euthanized via CO<sub>2</sub> inhalation followed by cervical dislocation. The embryos were transferred to sterile phosphate-buffered saline (PBS) on ice prior to processing for immunohistochemistry or cell culture.

### 4.2. Cryosectioning and immunohistochemistry

Pax3-Cre/ZsGreen1+ embryos were fixed in 4% paraformaldehyde (PFA) for 1 hr, washed with PBS 3×30 min before embedding in Optimal Cutting Temperature compound (OCT, Sakura Finetek). Embryos were then frozen in dry ice-cooled isopentane (Fisher Scientific) and stored at -80°C until sectioning. Serial, 10 µm-thick cryosections were collected and stored at -20°C. Before staining, sections were washed with PBS for 5 min to remove any residual OCT. Each section was fixed in 4% PFA for 5 min and rinsed with PBS. Then, sections were blocked for 30 min [blocking buffer: 10% donkey serum (Lampire), 0.2% bovine serum albumin, 0.02% sodium azide in PBS]. To label HA, biotinylated hyaluronic acid binding protein (HABP; 4µg/ml, Calbiochem, 385911) was used as described previously. Sections were incubated with HABP, and primary antibodies against RHAMM (33.3µg/ml, abcam, ab185728), CD44 (33.3µg/ml, Invitrogen, MA4405), Pax7 (13.3 µg/ml Developmental Studies Hybridoma Bank) and Tcf4 (50 µg/ml, Millipore, 05-511) at 4°C overnight, and washed with PBS for 3×5 min. Slides were blocked again for 10 min before staining with the appropriate secondary detection reagents [DyLight 550 anti-rat (1:250, Invitrogen), Alexa Fluor 546 anti-rabbit (1:500, Invitrogen), Alexa Fluor 546 Goat anti-Mouse IgG1 (1:500, Invitrogen), Alexa Fluor 647 anti-rabbit (1:500, Invitrogen), Alexa Fluor 647 Goat anti-Mouse IgG2a (1:500, Invitrogen), Alexa Fluor 647 streptavidin (1:500, Invitrogen), DAPI (1:500, Roche)] for 30 min. Sections were imaged at 5×, 10×, and 20×

using a Leica DMI6000 inverted microscope and at  $63\times$  using a Zeiss 800 confocal microscope. Images were acquired using the same imaging parameters across the different time points or treatments, and processed under identical conditions using ImageJ (NIH).

#### 4.3. Forelimb cell harvest and sorting

Forelimb buds from E10.5 - E12.5 Pax3-Cre/ZsGreen1+ embryos were removed with micro scissors. Forelimb buds from 2 – 3 animals were placed in a microcentrifuge tube, washed twice with PBS and incubated with 250 $\mu$ L pre-warmed 0.1% trypsin solution (2.5% HyClone trypsin protease, containing 0.2g/L EDTA, diluted with PBS) at 37°C for 5 min. Limb buds were dissociated by pipetting up and down using a 200  $\mu$ L tip. After inactivating the trypsin using growth medium [Dulbecco's modified Eagle's medium with L-glutamine (DMEM; Gibco) with L-glutamine, 10% fetal bovine serum (FBS; Gibco), 1% Pen/Strep/Fungiezone], the cell suspension was filtered through a 70 $\mu$ m strainer to remove large aggregates. Cells were centrifuged to remove the trypsin solution, resuspended in growth medium, stained with Trypan blue to identify dead cells and viable cells were counted by hemocytometer. To separate GFP+ and GFP- cells, samples were sorted using a FACS Aria III Cell Sorter (BD Biosciences, San Diego) at the Purdue University Center for Cancer Research (Bindley Bioscience Center). Isolated cells were expanded in culture for 2 days in DMEM+10%FBS growth medium, supplemented with 4ng/mL basic fibroblast growth factor (PeproTech), before performing the following assays.

#### 4.4. Cell culture

Cells were cultured *in vitro* using one of the following media: DMEM medium [DMEM with L-glutamine, 1% Pen/Strep/Fungiezone (HyClone)]; DMEM+10%FBS [DMEM with L-glutamine, 10% FBS, 1% Pen/Strep/Fungiezone], and adv DMEM [advanced DMEM (Gibco), 1% Pen/Strep/Fungiezone, 1% L- Glutagro (Corning) ] at 37°C in 5% CO<sub>2</sub>.

**4MU treatment:** 4-methylumbelliferone (4MU, Alfa Aesar) was dissolved in dimethyl sulfoxide (DMSO) to generate 0.5M and 1M stock solutions. For both migration and proliferation assays, cells were seeded on a 96-well plate at the density of  $2\times 10^4$  cells/cm<sup>2</sup> with 0mM, 0.5mM, or 1.0mM 4MU added to the growth medium, each having a final concentration of 0.1% DMSO.

**Antibody treatment:** Cells were seeded at  $2\times 10^4$  cells/cm<sup>2</sup> for 24 hrs before adding antibody-containing medium [100  $\mu$ g/mL of anti-CD44, anti-RHAMM, rat IgG2b (Invitrogen), and rabbit IgG (Invitrogen) isotype controls or cell growth medium alone (blank control)]. After confirming that there is no difference between the effect of rat IgG2b and rabbit IgG isotype controls in proliferation and migration assays, cells treated with rat IgG2b were used for normalization (denoted by IgG) in migration and proliferation studies, whereas for qPCR and ERK1/2 signaling, cells simultaneously treated with both isotype controls were used for normalization (denoted by IgGs).

#### 4.5. Quantitative RT-PCR

Total RNA was extracted from either freshly sorted E10.5-E12.5 forelimb GFP+/- cells or GFP+/- cells after 24 hrs antibody treatment using a RNeasy Mini Kit (QIAGEN) according

to the manufacturer's protocol. RNA concentrations were measured using a NanoDrop (Thermo Scientific), and nucleic acid purity was monitored by confirming the A260:A280 ratio was ~2.0. Equal amounts of total RNA were reverse-transcribed with a iScript cDNA synthesis kit (Bio-Rad). cDNA generated from 3 ng of RNA was combined with primers for genes of interest (Table 1) and SsoAdvanced Universal SYBR Green Supermix (Bio-Rad). Quantitative PCR was performed using a CFX96 real-time thermal cycler (Bio-Rad) with a program of 3 min at 95°C for enzyme activation, followed by 40 cycles with 10 s denaturing at 95°C and 30 s at 54°C or 55°C (depending on the primer pair) for annealing. The presence of single amplicons was validated by performing a melt-curve analysis. Target genes were normalized to the housekeeping gene  $\beta$ -actin. Expression of  $\beta$ -actin was constant across the time points investigated in this study. Fold change in gene expression was calculated by determining Cq values.

#### 4.6. Cell migration assay

The influence of 4MU or anti-CD44 and anti-RHAMM antibodies on the migration of GFP+ and GFP- cells was determined by imaging cultures every hour for 24 hrs at 37°C, 5% CO<sub>2</sub> on a Leica DMI6000 fluorescence live cell microscope. The total distance individual cells traveled was determined by using the Manual Tracking plugin in ImageJ. For each biological replicate, the influence of individual treatments on migration was averaged from three wells. The results are presented as a mean of n = 3 biological replicates  $\pm$  S.E.

#### 4.7. Cell proliferation assay

To analyze proliferation, cells cultured with either 4MU or antibodies were incubated with 5 $\mu$ M 5- ethynyl-2'-deoxyuridine (EdU; ThermoFisher) for 24 hrs. 10 mM EdU stock solution was prepared in DMSO, then further diluted in growth medium to 5 $\mu$ M. Cells were fixed and stained for EdU incorporation using a ThermoFisher Click-iT Plus EdU kit and co-stained with DAPI. Proliferation was expressed as the percentage of EdU+ nuclei relative to the total number of nuclei analyzed. For each biological replicate, the influence of individual treatments on proliferation was averaged from three wells. The results are presented as a mean of n = 3 biological replicates  $\pm$  S.D.

#### 4.8. Analysis of ERK1,2 Activation

For quantification of serum induced ERK1,2 activation after antibody treatment, isolated GFP+ cells were seeded on a 96 well plate for at least one day, serum starved for 5 hrs, incubated with primary antibodies as described above for 30 min then stimulated with 10% FBS by directly adding FBS to cultures. An ELISA for ERK1,2 (abcam) was carried out according to the manufacturer's instructions. For each biological replicate, the influence of individual treatments on ERK1,2 phosphorylation was averaged from three wells. The results are presented as a mean of n = 3 biological replicates  $\pm$  S.D. The ratio of phospho-ERK1,2 protein to total ERK1,2 protein was normalized by IgGs control.

#### 4.9. Transduction of cells with scrambled shRNA, shCD44 or shRHAMM

Depletion of CD44 and RHAMM expression was achieved through TRC lentiviral-mediated transduction of TRCN0000065355 (shCD44-1), TRCN0000065357 (shCD44-2),



TRCN0000071588 (shRHAMM-1), TRCN0000071590 (shRHAMM-2), TRCN0000071592 (shRHAMM-3), or a scrambled control shRNA (GE Dharmacon, Lafayette, CO). Plasmid preparation and replication were conducted following the manufacturer's instructions. Lentiviral particles were produced in HEK-293 cells upon cotransfection with pMD2.G and psPAX2. Viral particle-containing supernatants were diluted 1:1 in growth medium. GFP+ and GFP-cells were transduced with lentiviral particles for 48 hrs in the presence of 5 µg/mL polybrene. After transduction, cells were allowed to recover for 24 hrs. In all cases, stable genomic integration of constructs was selected for using 1.25µg/mL puromycin (Sigma-Aldrich, St. Louis, MI) for 10 days before conducting migration or proliferation assays. Gene depletion was verified by immunoblotting with antibodies against CD44 and RHAMM and qPCR.

#### 4.10. Western blot analysis

Cells were lysed using a modified RIPA lysis buffer containing 50 mM Tris, 150mM NaCl, 0.25% sodium deoxycholate, 1.0% NP40, 0.1% SDS, 10mM activated sodium orthovanadate, 40 mM β- glycerolphosphate, 20mM sodium fluoride and protease inhibitor cocktail (Sigma Aldrich, St.Louis, MO). The concentration of protein was determined using the Pierce BCA Protein Assay (ThermoFisher Scientific, Rockford, IL). Protein samples were mixed with 4x laemmli buffer and denatured by incubation at 98 °C for 5min. Lysates were separated by reducing SDS P.A.G.E. and transferred to PVDF membranes (Bio-Rad). The PVDF membrane was soaked in methanol, air-dried and incubated with CD44 (ThermoFisher Scientific, Rockford, IL), RHAMM (Abcam, Cambridge, MA) or β-tubulin (DSHB, Iowa City, IA) in 5% milk in TBST (10X Tris Buffered Saline with Tween 20) at 4C overnight. Membranes were incubated with HRP-coupled secondary antibodies (Sigma Aldrich, St.Louis, MO) for one hour at room temperature. The membranes were washed with TBST and chemiluminescence was detected using home-made ECL Substrate. Image Lab 2017 Version 6.0 (Bio-Rad) was used to quantify western blot bands.

#### 4.11. Statistical analysis

Prism 7.0 (GraphPad Software, La Jolla, CA) were used for statistical analysis. One-way ANOVA and two-way ANOVA, followed by Tukey's post hoc analysis ( $\alpha = 0.05$ ) were used to analyze qPCR, migration, proliferation and ERK ELISA data. Error bars represent the S.E. or S.D. as indicated. Data were normalized by the control (as indicated in each figure) before statistical analyses were performed. A 95% confidence interval was accepted, and adjusted p value was reported, where  $0.01 < p < 0.05$  was deemed significant (\*),  $0.001 < p < 0.01$  was deemed very significant (\*\*), and  $p < 0.001$  was deemed extremely significant (\*\*\*).

### Supplementary Material

Refer to Web version on PubMed Central for supplementary material.

### Acknowledgments

The authors would like to thank Dr. David Umulis for the use of his confocal, and Dr. Shihuan Kuang for advice on study design.

## 5. Funding

This work was supported by the National Institutes of Health [R03 AR065201, R01 AR071359 and DP2 AT009833 to S.C.] and the Ralph W. and Grace M. Showalter Research Trust.

### Funding

This work was supported by the National Institutes of Health [R03 AR065201, R01 AR071359 and DP2 AT009833 to S.C.] and the Ralph W. and Grace M. Showalter Research Trust.

## Abbreviations:

<b>4MU</b>	4-methylumbelliferone
<b>CD44</b>	cluster of differentiation 44
<b>EdU</b>	5-ethynyl-2'-deoxyuridine
<b>ERK1/2</b>	extracellular signal-regulated kinase 1/2
<b>GFP</b>	green fluorescent protein
<b>HA</b>	hyaluronic acid
<b>HAS</b>	hyaluronic acid synthase
<b>HYAL</b>	hyaluronidase
<b>RHAMM</b>	receptor for hyaluronan-mediated motility

## 9. References

- [1]. Buckingham M, Bajard L, Chang T, Daubas P, Hadchouel J, Meilhac S, Montarras D, Rocancourt D, Relaix F, The formation of skeletal muscle: from somite to limb, *J. Anat.* 202 (2003) 59–68. <http://www.ncbi.nlm.nih.gov/pubmed/12587921>. [PubMed: 12587921]
- [2]. Biressi S, Molinaro M, Cossu G, Cellular heterogeneity during vertebrate skeletal muscle development, *Dev. Biol.* 308 (2007) 281–93. doi:10.1016/j.ydbio.2007.06.006. [PubMed: 17612520]
- [3]. Chargé SBP, Rudnicki MA, Cellular and molecular regulation of muscle regeneration, *Physiol. Rev.* 84 (2004) 209–38. doi:10.1152/physrev.00019.2003. [PubMed: 14715915]
- [4]. Vallecillo-Garcia P, Orgeur M, vom Hofe-Schneider S, Stumm J, Kappert V, Ibrahim DM, Borno ST, Hayashi S, Relaix F, Hildebrandt K, Sengle G, Koch M, Timmermann B, Marazzi G, Sassoon DA, Duprez D, Stricker S, Odd skipped-related 1 identifies a population of embryonic fibro-adipogenic progenitors regulating myogenesis during limb development, *Nat. Commun.* 8 (2017) 1218. doi:10.1038/s41467-017-01120-3. [PubMed: 29084951]
- [5]. Mathew SJ, Hansen JM, Merrell AJ, Murphy MM, Lawson JA, Hutcheson DA, Hansen MS, Angus-Hill M, Kardon G, Connective tissue fibroblasts and Tcf4 regulate myogenesis, *Development.* 138 (2011) 371–84. doi:10.1242/dev.057463. [PubMed: 21177349]
- [6]. Grounds MD, Complexity of Extracellular Matrix and Skeletal Muscle Regeneration, in: *Skelet. Muscle Repair Regen*, Springer Netherlands, Dordrecht, 2008: pp. 269–302. doi: 10.1007/978-1-4020-6768-6\_13.
- [7]. Bosman FT, Stamenkovic I, Functional structure and composition of the extracellular matrix, *J. Pathol.* 200 (2003) 423–428. doi:10.1002/path.1437. [PubMed: 12845610]

- [8]. Sanes JR, The basement membrane/basal lamina of skeletal muscle, *J. Biol. Chem.* 278 (2003) 12601–4. doi:10.1074/jbc.R200027200. [PubMed: 12556454]
- [9]. Calve S, Odelberg SJ, Simon HG, A transitional extracellular matrix instructs cell behavior during muscle regeneration, *Dev. Biol.* 344 (2010) 259–71. doi:10.1016/j.ydbio.2010.05.007. [PubMed: 20478295]
- [10]. Okita M, Yoshimura T, Nakano J, Motomura M, Eguchi K, Effects of reduced joint mobility on sarcomere length, collagen fibril arrangement in the endomysium, and hyaluronan in rat soleus muscle, *J. Muscle Res. Cell Motil.* 25 (2004) 159–66. <http://www.ncbi.nlm.nih.gov/pubmed/15360131>. [PubMed: 15360131]
- [11]. Calve S, Isaac J, Gumucio JP, Mendias CL, Hyaluronic acid, HAS1, and HAS2 are significantly upregulated during muscle hypertrophy, *Am. J. Physiol. Cell Physiol.* 303 (2012) C577–88. doi:10.1152/ajpcell.00057.2012. [PubMed: 22785117]
- [12]. Solis MA, Chen YH, Wong TY, Bittencourt VZ, Lin YC, Huang LLH, Hyaluronan regulates cell behavior: a potential niche matrix for stem cells, *Biochem. Res. Int.* 2012 (2012) 346972. doi:10.1155/2012/346972. [PubMed: 22400115]
- [13]. Spicer AP, Tien JYL, Hyaluronan and morphogenesis, *Birth Defects Res. C. Embryo Today.* 72 (2004) 89–108. doi:10.1002/bdrc.20006. [PubMed: 15054906]
- [14]. Matsumoto K, Li Y, Jakuba C, Sugiyama Y, Sayo T, Okuno M, Dealy CN, Toole BP, Takeda J, Yamaguchi Y, Kosher RA, Conditional inactivation of Has2 reveals a crucial role for hyaluronan in skeletal growth, patterning, chondrocyte maturation and joint formation in the developing limb, *Development.* 136 (2009) 2825–35. doi:10.1242/dev.038505. [PubMed: 19633173]
- [15]. Camenisch TD, Spicer AP, Brehm-Gibson T, Biesterfeldt J, Augustine ML, Calabro A, Kubalak S, Klewer SE, McDonald JA, McDonald JA, Disruption of hyaluronan synthase-2 abrogates normal cardiac morphogenesis and hyaluronan-mediated transformation of epithelium to mesenchyme, *J. Clin. Invest.* 106 (2000) 349–60. doi:10.1172/JCI10272. [PubMed: 10930438]
- [16]. Knudson CB, Hyaluronan and CD44: Strategic players for cell-matrix interactions during chondrogenesis and matrix assembly, *Birth Defects Res. Part C Embryo Today Rev.* 69 (2003) 174–196. doi:10.1002/bdrc.10013.
- [17]. Dicker KT, Gurski LA, Pradhan-Bhatt S, Witt RL, Farach-Carson MC, Jia X, Hyaluronan: a simple polysaccharide with diverse biological functions, *Acta Biomater.* 10 (2014) 1558–70. doi:10.1016/j.actbio.2013.12.019. [PubMed: 24361428]
- [18]. Toole BP, Hyaluronan: from extracellular glue to pericellular cue, *Nat. Rev. Cancer.* 4 (2004) 528–39. doi:10.1038/nrc1391. [PubMed: 15229478]
- [19]. Itano N, Simple primary structure, complex turnover regulation and multiple roles of hyaluronan, *J. Biochem.* 144 (2008) 131–7. doi:10.1093/jb/mvn046. [PubMed: 18390876]
- [20]. Tolg C, Yuan H, Flynn SM, Basu K, Ma J, Tse KCK, Kowalska B, Vulkanesku D, Cowman MK, McCarthy JB, Turley EA, Hyaluronan modulates growth factor induced mammary gland branching in a size dependent manner, *Matrix Biol.* 63 (2017) 117–132. doi:10.1016/j.matbio.2017.02.003. [PubMed: 28232112]
- [21]. Toole BP, Hyaluronan in morphogenesis, *Semin. Cell Dev. Biol.* 12 (2001) 79–87. doi:10.1006/scdb.2000.0244. [PubMed: 11292373]
- [22]. Aruffo A, Stamenkovic I, Melnick M, Underhill CB, Seed B, CD44 is the principal cell surface receptor for hyaluronate, *Cell.* 61 (1990) 1303–13. <http://www.ncbi.nlm.nih.gov/pubmed/1694723>. [PubMed: 1694723]
- [23]. Turley EA, Noble PW, Bourguignon LYW, Signaling properties of hyaluronan receptors, *J. Biol. Chem.* 277 (2002) 4589–92. doi:10.1074/jbc.R100038200. [PubMed: 11717317]
- [24]. Hardwick C, Hoare K, Owens R, Hohn HP, Hook M, Moore D, Cripps V, Austen L, Nance DM, Turley EA, Molecular cloning of a novel hyaluronan receptor that mediates tumor cell motility, *J. Cell Biol.* 117 (1992) 1343–50. <http://www.ncbi.nlm.nih.gov/pubmed/1376732>. [PubMed: 1376732]
- [25]. Dzwonek J, Wilczynski GM, CD44: molecular interactions, signaling and functions in the nervous system, *Front. Cell. Neurosci.* 9 (2015) 175. doi:10.3389/fncel.2015.00175. [PubMed: 25999819]

- [26]. Ponta H, Sherman L, Herrlich PA, CD44: from adhesion molecules to signalling regulators, *Nat. Rev. Mol. Cell Biol.* 4 (2003) 33–45. doi:10.1038/nrm1004. [PubMed: 12511867]
- [27]. Isacke CM, Yarwood H, The hyaluronan receptor, CD44, *Int. J. Biochem. Cell Biol.* 34 (2002) 718–21. <http://www.ncbi.nlm.nih.gov/pubmed/11950588>. [PubMed: 11950588]
- [28]. Lesley J, Hyman R, Kincade PW, CD44 and its interaction with extracellular matrix, *Adv. Immunol.* 54 (1993) 271–335. <http://www.ncbi.nlm.nih.gov/pubmed/8379464>. [PubMed: 8379464]
- [29]. Misra S, Hascall VC, Markwald RR, Ghatak S, Interactions between Hyaluronan and Its Receptors (CD44, RHAMM) Regulate the Activities of Inflammation and Cancer, *Front. Immunol.* 6 (2015) 201. doi:10.3389/fimmu.2015.00201. [PubMed: 25999946]
- [30]. Maleski MP, Knudson CB, Hyaluronan-Mediated Aggregation of Limb Bud Mesenchyme and Mesenchymal Condensation during Chondrogenesis, *Exp. Cell Res.* 225 (1996) 55–66. doi:10.1006/excr.1996.0156. [PubMed: 8635517]
- [31]. Kaya G, Rodriguez I, Jorcano JL, Vassalli P, Stamenkovic I, Selective suppression of CD44 in keratinocytes of mice bearing an antisense CD44 transgene driven by a tissue-specific promoter disrupts hyaluronate metabolism in the skin and impairs keratinocyte proliferation, *Genes Dev.* 11 (1997) 996–1007. <http://www.ncbi.nlm.nih.gov/pubmed/9136928>. [PubMed: 9136928]
- [32]. Knudson W, Chow G, Knudson CB, CD44-mediated uptake and degradation of hyaluronan, *Matrix Biol.* 21 (2002) 15–23. doi:10.1016/S0945-053X(01)00186-X. [PubMed: 11827788]
- [33]. Maxwell CA, McCarthy J, Turley E, Cell-surface and mitotic-spindle RHAMM: moonlighting or dual oncogenic functions?, *J. Cell Sci.* 121 (2008) 925–32. doi:10.1242/jcs.022038. [PubMed: 18354082]
- [34]. Yang B, Yang BL, Savani RC, Turley EA, Identification of a common hyaluronan binding motif in the hyaluronan binding proteins RHAMM, CD44 and link protein, *EMBO J.* 13 (1994) 286–96. <http://www.ncbi.nlm.nih.gov/pubmed/7508860>. [PubMed: 7508860]
- [35]. Tolg C, McCarthy JB, Yazdani A, Turley EA, Hyaluronan and RHAMM in wound repair and the “cancerization” of stromal tissues, *Biomed Res. Int.* 2014 (2014) 103923. doi:10.1155/2014/103923. [PubMed: 25157350]
- [36]. Assmann V, Jenkinson D, Marshall JF, Hart IR, The intracellular hyaluronan receptor RHAMM/IHABP interacts with microtubules and actin filaments, *J. Cell Sci.* (1999) 3943–54. <http://www.ncbi.nlm.nih.gov/pubmed/10547355>. [PubMed: 10547355]
- [37]. Silverman-Gavrila R, Silverman-Gavrila L, Hou G, Zhang M, Charlton M, Bendek MP, Rear Polarization of the Microtubule-Organizing Center in Neointimal Smooth Muscle Cells Depends on PKCa, ARPC5, and RHAMM, *Am. J. Pathol.* 178 (2011) 895–910. doi:10.1016/J.AJPAT.2010.10.001. [PubMed: 21281821]
- [38]. Schmits R, Filmus J, Gerwin N, Senaldi G, Kiefer F, Kundig T, Wakeham A, Shahinian A, Catzavelos C, Rak J, Furlonger C, Zakarian A, Simard JJ, Ohashi PS, Paige CJ, Gutierrez-Ramos JC, Mak TW, CD44 regulates hematopoietic progenitor distribution, granuloma formation, and tumorigenicity, *Blood.* 90 (1997) 2217–33. <http://www.ncbi.nlm.nih.gov/pubmed/9310473>. [PubMed: 9310473]
- [39]. Nedvetzki S, Gonen E, Assayag N, Reich R, Williams RO, Thurmond RL, Huang JF, Neudecker BA, Wang FS, Wang FS, Turley EA, Naor D, RHAMM, a receptor for hyaluronan-mediated motility, compensates for CD44 in inflamed CD44-knockout mice: a different interpretation of redundancy, *Proc. Natl. Acad. Sci. U. S. A.* 101 (2004) 18081–6. doi:10.1073/pnas.0407378102. [PubMed: 15596723]
- [40]. Tolg C, Poon R, Fodde R, Turley EA, Alman BA, Genetic deletion of receptor for hyaluronan-mediated motility (Rhamm) attenuates the formation of aggressive fibromatosis (desmoid tumor), *Oncogene.* 22 (2003) 6873–82. doi:10.1038/sj.onc.1206811. [PubMed: 14534534]
- [41]. Mylona E, Jones KA, Mills ST, Pavlath GK, CD44 regulates myoblast migration and differentiation, *J. Cell. Physiol.* 209 (2006) 314–21. doi:10.1002/jcp.20724. [PubMed: 16906571]
- [42]. Goueffic Y, Guilluy C, Guerin P, Patra P, Pacaud P, Loirand G, Hyaluronan induces vascular smooth muscle cell migration through RHAMM-mediated PI3K-dependent Rac activation, *Cardiovasc. Res.* 72 (2006) 339–348. doi:10.1016/j.cardiores.2006.07.017. [PubMed: 16934786]

- [43]. Tolg C, Hamilton SR, Nakrieko KA, Kooshesh F, Walton P, McCarthy JB, Bissell MJ, Turley EA, Rhamm-/- fibroblasts are defective in CD44-mediated ERK1,2 mitogenic signaling, leading to defective skin wound repair, *J. Cell Biol.* 175 (2006) 1017–28. doi:10.1083/jcb.200511027. [PubMed: 17158951]
- [44]. Hunt LC, Gorman C, Kintakas C, McCulloch DR, Mackie EJ, White JD, Hyaluronan synthesis and myogenesis: a requirement for hyaluronan synthesis during myogenic differentiation independent of pericellular matrix formation, *J. Biol. Chem.* 288 (2013) 13006–21. doi:10.1074/jbc.M113.453209. [PubMed: 23493399]
- [45]. Hutcheson DA, Zhao J, Merrell A, Haldar M, Kardon G, Embryonic and fetal limb myogenic cells are derived from developmentally distinct progenitors and have different requirements for beta-catenin, *Genes Dev.* 23 (2009) 997–1013. doi:10.1101/gad.1769009. [PubMed: 19346403]
- [46]. Spicer AP, McDonald JA, Characterization and molecular evolution of a vertebrate hyaluronan synthase gene family, *J. Biol. Chem.* 273 (1998) 1923–32. <http://www.ncbi.nlm.nih.gov/pubmed/9442026>. [PubMed: 9442026]
- [47]. Kakizaki I, Kojima K, Takagaki K, Endo M, Kannagi R, Ito M, Maruo Y, Sato H, Yasuda T, Mita S, Kimata K, Itano N, A novel mechanism for the inhibition of hyaluronan biosynthesis by 4-methylumbelliferone, *J. Biol. Chem.* 279 (2004) 33281–9. doi:10.1074/jbc.M405918200. [PubMed: 15190064]
- [48]. Vignetti D, Rizzi M, Viola M, Karousou E, Genasetti A, Clerici M, Bartolini B, Hascall VC, De Luca G, Passi A, The effects of 4-methylumbelliferone on hyaluronan synthesis, MMP2 activity, proliferation, and motility of human aortic smooth muscle cells, *Glycobiology.* 19 (2009) 537–46. doi: 10.1093/glycob/cwp022. [PubMed: 19240269]
- [49]. Pilarski LM, Masellis-Smith A, Belch AR, Yang B, Savani RC, Turley EA, RHAMM, a receptor for hyaluronan-mediated motility, on normal human lymphocytes, thymocytes and malignant B cells: a mediator in B cell malignancy?, *Leuk. Lymphoma.* 14 (1994) 363–74. doi: 10.3109/10428199409049691. [PubMed: 7529076]
- [50]. Salic A, Mitchison TJ, A chemical method for fast and sensitive detection of DNA synthesis *in vivo*, *Proc. Natl. Acad. Sci. U. S. A.* 105 (2008) 2415–20. doi:10.1073/pnas.0712168105. [PubMed: 18272492]
- [51]. Hatano H, Shigeishi H, Kudo Y, Higashikawa K, Tobiume K, Takata T, Kamata N, RHAMM/ERK interaction induces proliferative activities of cementifying fibroma cells through a mechanism based on the CD44-EGFR, *Lab. Invest.* 91 (2011) 379–91. doi:10.1038/labinvest.2010.176. [PubMed: 20956971]
- [52]. Takahashi Y, Li L, Kamiryo M, Asteriou T, Moustakas A, Yamashita H, Heldin P, Hyaluronan fragments induce endothelial cell differentiation in a CD44- and CXCL1/GRO1- dependent manner, *J. Biol. Chem.* 280 (2005) 24195–204. doi:10.1074/jbc.M411913200. [PubMed: 15843382]
- [53]. Bourguignon LYW, Gilad E, Peyrollier K, Heregulin-mediated ErbB2-ERK signaling activates hyaluronan synthases leading to CD44-dependent ovarian tumor cell growth and migration, *J. Biol. Chem.* 282 (2007) 19426–41. doi:10.1074/jbc.M610054200. [PubMed: 17493932]
- [54]. Acharya PS, Majumdar S, Jacob M, Hayden J, Mrass P, Weninger W, Assoian RK, Puré E, Fibroblast migration is mediated by CD44-dependent TGF beta activation, *J. Cell Sci.* 121 (2008) 1393–402. doi: 10.1242/jcs.021683. [PubMed: 18397995]
- [55]. Campbell AL, Shih HP, Xu J, Gross MK, Kioussi C, Regulation of Motility of Myogenic Cells in Filling Limb Muscle Anlagen by Pitx2, *PLoS One.* 7 (2012) e35822. doi :10.1371/journal.pone.0035822. [PubMed: 22558231]
- [56]. Hatano H, Shigeishi H, Kudo Y, Higashikawa K, Tobiume K, Takata T, Kamata N, Overexpression of receptor for hyaluronan-mediated motility (RHAMM) in MC3T3-E1 cells induces proliferation and differentiation through phosphorylation of ERK1/2, *J. Bone Miner. Metab.* 30 (2012) 293–303. doi:10.1007/s00774-011-0318-0. [PubMed: 21947782]
- [57]. Hilberg F, Protin U, Schweighoffer T, Jochum W, CD44-Deficient Mice Develop Normally with Changes in Subpopulations and Recirculation of Lymphocyte Subsets, *J Immunol Ref.* 4917 (2018)4917–4923. <http://www.jimmunol.org/content/163/9/http://www.jimmunol.org/content/163/9/4917.full#ref-list-1>.

- [58]. Sherman L, Wainwright D, Ponta H, Herrlich P, A splice variant of CD44 expressed in the apical ectodermal ridge presents fibroblast growth factors to limb mesenchyme and is required for limb outgrowth, *Genes Dev.* 12 (1998) 1058–71. <http://www.ncbi.nlm.nih.gov/pubmed/9531542>. [PubMed: 9531542]
- [59]. Midgley AC, Rogers M, Hallett MB, Clayton A, Bowen T, Phillips AO, Steadman R, Transforming Growth Factor- $\beta$ 1 (TGF- $\beta$ 1)-stimulated Fibroblast to Myofibroblast Differentiation Is Mediated by Hyaluronan (HA)-facilitated Epidermal Growth Factor Receptor (EGFR) and CD44 Co-localization in Lipid Rafts, *J. Biol. Chem.* 288 (2013) 14824–14838. doi:10.1074/jbc.M113.451336. [PubMed: 23589287]
- [60]. Jacobson A, Brinck J, Briskin MJ, Spicer AP, Heldin P, Expression of human hyaluronan synthases in response to external stimuli, *Biochem. J.* 348 Pt 1 (2000) 29–35. <http://www.ncbi.nlm.nih.gov/pubmed/10794710>. [PubMed: 10794710]
- [61]. Wang Y, Lauer ME, Anand S, Mack JA, Maytin EV, Hyaluronan synthase 2 protects skin fibroblasts against apoptosis induced by environmental stress, *J. Biol. Chem.* 289 (2014) 32253–65. doi: 10.1074/jbc.M114.578377. [PubMed: 25266724]
- [62]. Tien JYL, Spicer AP, Three vertebrate hyaluronan synthases are expressed during mouse development in distinct spatial and temporal patterns, *Dev. Dyn.* 233 (2005) 130–141. doi: 10.1002/dvdy.20328. [PubMed: 15765504]
- [63]. Adamia S, Maxwell CA, Pilarski LM, Hyaluronan and hyaluronan synthases: potential therapeutic targets in cancer, *Curr. Drug Targets. Cardiovasc. Haematol. Disord.* 5 (2005) 3–14. <http://www.ncbi.nlm.nih.gov/pubmed/15720220>. [PubMed: 15720220]
- [64]. Brinck J, Heldin P, Expression of Recombinant Hyaluronan Synthase (HAS) Isoforms in CHO Cells Reduces Cell Migration and Cell Surface CD44, *Exp. Cell Res.* 252 (1999) 342–351. doi: 10.1006/excr.1999.4645. [PubMed: 10527624]
- [65]. Fraser JR, Laurent TC, Laurent UB, Hyaluronan: its nature, distribution, functions and turnover, *J. Intern. Med.* 242 (1997) 27–33. <http://www.ncbi.nlm.nih.gov/pubmed/9260563>. [PubMed: 9260563]
- [66]. Ghatak S, Maytin EV, Mack JA, Hascall VC, Atanelishvili I, Moreno Rodriguez R, Markwald RR, Misra S, Roles of Proteoglycans and Glycosaminoglycans in Wound Healing and Fibrosis, *Int. J. Cell Biol.* 2015 (2015) 1–20. doi: 10.1155/2015/834893.
- [67]. Clarkin CE, Allen S, Wheeler-Jones CP, Bastow ER, Pitsillides AA, Reduced chondrogenic matrix accumulation by 4-methylumbelliferone reveals the potential for selective targeting of UDP-glucose dehydrogenase, *Matrix Biol.* 30 (2011) 163–168. doi:10.1016/j.matbio.2011.01.002. [PubMed: 21292001]
- [68]. Lokeshwar VB, Lopez LE, Munoz D, Chi A, Shirodkar SP, Lokeshwar SD, Escudero DO, Dhir N, Altman N, Antitumor activity of hyaluronic acid synthesis inhibitor 4-methylumbelliferone in prostate cancer cells, *Cancer Res.* 70 (2010) 2613–23. doi:10.1158/0008-5472.CAN-09-3185. [PubMed: 20332231]
- [69]. Twarock S, Freudenberger T, Poscher E, Dai G, Jannasch K, Dullin C, Alves F, Prenzel K, Knoefel WT, Stoecklein NH, Savani RC, Homey B, Fischer JW, Inhibition of oesophageal squamous cell carcinoma progression by *in vivo* targeting of hyaluronan synthesis, *Mol. Cancer.* 10 (2011) 30. doi: 10.1186/1476-4598-10-30. [PubMed: 21429221]
- [70]. Urakawa H, Nishida Y, Wasa J, Arai E, Zhuo L, Kimata K, Kozawa E, Futamura N, Ishiguro N, Inhibition of hyaluronan synthesis in breast cancer cells by 4-methylumbelliferone suppresses tumorigenicity *in vitro* and metastatic lesions of bone *in vivo*, *Int. J. Cancer.* 130 (2012) 454–66. doi:10.1002/ijc.26014. [PubMed: 21387290]
- [71]. Jong A, Wu CH, Gonzales-Gomez I, Kwon-Chung KJ, Chang YC, Tseng HK, Cho WL, Huang SH, Hyaluronic acid receptor CD44 deficiency is associated with decreased *Cryptococcus neoformans* brain infection, *J. Biol. Chem.* 287 (2012) 15298–306. doi:10.1074/jbc.M112.353375. [PubMed: 22418440]
- [72]. Zhang S, Chang MC, Zylka D, Turley S, Harrison R, Turley EA, The hyaluronan receptor RHAMM regulates extracellular-regulated kinase, *J. Biol. Chem.* 273 (1998) 11342–8. <http://www.ncbi.nlm.nih.gov/pubmed/9556628>. [PubMed: 9556628]
- [73]. Tolg C, Hamilton SR, Morningstar L, Zhang J, Zhang S, V Esguerra K, Telmer PG, Luyt LG, Harrison R, McCarthy JB, Turley EA, RHAMM promotes interphase microtubule instability and



- mitotic spindle integrity through MEK1/ERK1/2 activity, *J. Biol. Chem.* 285 (2010) 26461–74. doi:10.1074/jbc.M110.121491. [PubMed: 20558733]
- [74]. Rudzki Z, Jothy S, CD44 and the adhesion of neoplastic cells, *Mol. Pathol.* 50 (1997) 57–71. doi: 10.1136/MP.50.2.57. [PubMed: 9231152]
- [75]. Goodison S, Urquidí V, Tarin D, CD44 cell adhesion molecules, *Mol. Pathol.* 52 (1999) 189–96. <http://www.ncbi.nlm.nih.gov/pubmed/10694938>. [PubMed: 10694938]
- [76]. Huang M, Sun R, Wei H, Tian Z, Simultaneous Knockdown of Multiple Ligands of Innate Receptor NKG2D Prevents Natural Killer Cell-Mediated Fulminant Hepatitis in Mice, *Hepatology.* 57 (2013) 277–88. doi: 10.1002/hep.25959. [PubMed: 22806577]
- [77]. Faassen AE, Schrage JA, Klein DJ, Oegema TR, Couchman JR, McCarthy JB, A cell surface chondroitin sulfate proteoglycan, immunologically related to CD44, is involved in type I collagen-mediated melanoma cell motility and invasion, *J. Cell Biol.* 116 (1992) 521–31. <http://www.ncbi.nlm.nih.gov/pubmed/1730766>. [PubMed: 1730766]
- [78]. Radotra B, McCormick D, Crockard A, CD44 plays a role in adhesive interactions between glioma cells and extracellular matrix components, *Neuropathol. Appl. Neurobiol.* 20 (1994) 399–405. doi: 10.1111/j.1365-2990.1994.tb00986.x. [PubMed: 7528901]
- [79]. Jalkanen S, Jalkanen M, Lymphocyte CD44 binds the COOH-terminal heparin-binding domain of fibronectin, *J. Cell Biol.* 116 (1992) 817–25. <http://www.ncbi.nlm.nih.gov/pubmed/1730778>. [PubMed: 1730778]
- [80]. Hibino S, Shibuya M, Hoffman MP, Engbring JA, Hossain R, Mochizuki M, Kudoh S, Nomizu M, Kleinman HK, Laminin  $\alpha 5$  Chain Metastasis- and Angiogenesis-Inhibiting Peptide Blocks Fibroblast Growth Factor 2 Activity by Binding to the Heparan Sulfate Chains of CD44, *Cancer Res.* 65 (2005) 10494–10501. doi:10.1158/0008-5472.CAN-05-0314. [PubMed: 16288042]
- [81]. Hurt-Camejo E, Rosengren B, Sartipy P, Elfsberg K, Camejo G, Svensson L, CD44, a cell surface chondroitin sulfate proteoglycan, mediates binding of interferon-gamma and some of its biological effects on human vascular smooth muscle cells, *J. Biol. Chem.* 274 (1999) 18957–64. <http://www.ncbi.nlm.nih.gov/pubmed/10383394>. [PubMed: 10383394]
- [82]. Subhra Mohapatra B, AWright J, Turley EA, Greenberg AH, Soluble Hyaluronan Receptor RHAMM Induces Mitotic Arrest by Suppressing Cdc2 and Cyclin B1 Expression, *J Exp Med.* 183 (1996) 1663–1668. doi:10.1084/jem.183.4.1663. [PubMed: 8666924]
- [83]. Savani RC, Cao G, Pooler PM, Zaman A, Zhou Z, DeLisser HM, Differential involvement of the hyaluronan (HA) receptors CD44 and receptor for HA-mediated motility in endothelial cell function and angiogenesis, *J. Biol. Chem.* 276 (2001) 36770–8. doi:10.1074/jbc.M102273200. [PubMed: 11448954]
- [84]. Masellis-Smith A, Belch A, Mant M, Turley E, Pilarski L, Hyaluronan-dependent motility of B cells and leukemic plasma cells in blood, but not of bone marrow plasma cells, in multiple myeloma: alternate use of receptor for hyaluronan-mediated motility (RHAMM) and CD44, *Blood.* 87 (1996). [http://www.bloodjournal.org/content/87/5/1891?ijkey=686355dd0fcfd6c8cda7723ddc0cf71256b454e0&keytype=tf\\_ipsecsha](http://www.bloodjournal.org/content/87/5/1891?ijkey=686355dd0fcfd6c8cda7723ddc0cf71256b454e0&keytype=tf_ipsecsha).
- [85]. Hamilton SR, Fard SF, Paiwand FF, Tolg C, Veiseh M, Wang C, McCarthy JB, Bissell MJ, Koropatnick J, Turley EA, The hyaluronan receptors CD44 and Rhamm (CD168) form complexes with ERK1,2 that sustain high basal motility in breast cancer cells, *J. Biol. Chem.* 282 (2007) 16667–80. doi:10.1074/jbc.M702078200. [PubMed: 17392272]
- [86]. Engleka KA, Gitler AD, Zhang M, Zhou DD, High FA, Epstein JA, Insertion of Cre into the Pax3 locus creates a new allele of Splotch and identifies unexpected Pax3 derivatives, *Dev. Biol.* 280 (2005) 396–406. doi:10.1016/j.ydbio.2005.02.002. [PubMed: 15882581]
- [87]. Soriano P, Generalized lacZ expression with the ROSA26 Cre reporter strain, *Nat. Genet.* 21 (1999) 70–71. doi: 10.1038/5007. [PubMed: 9916792]
- [88]. Colasanto MP, Eyal S, Mohassel P, Bamshad M, Bonnemann CG, Zelzer E, Moon AM, Kardon G, Development of a subset of forelimb muscles and their attachment sites requires the ulnar-mammary syndrome gene *Tbx3*, *Dis. Model. Mech.* 9 (2016) 1257–1269. doi:10.1242/dmm.025874. [PubMed: 27491074]

- [89]. Murphy MM, Lawson JA, Mathew SJ, Hutcheson DA, Kardon G, Satellite cells, connective tissue fibroblasts and their interactions are crucial for muscle regeneration, *Development*. 138 (2011) 3625–37. doi:10.1242/dev.064162. [PubMed: 21828091]

Author Manuscript

Author Manuscript

Author Manuscript

Author Manuscript

**Highlights**

- CD44, RHAMM and HA expression temporally varied during forelimb development
- shRNA-mediated depletion of CD44 and RHAMM inhibited proliferation and migration
- Antibody blocking of CD44 and RHAMM had a differential effect than shRNA depletion

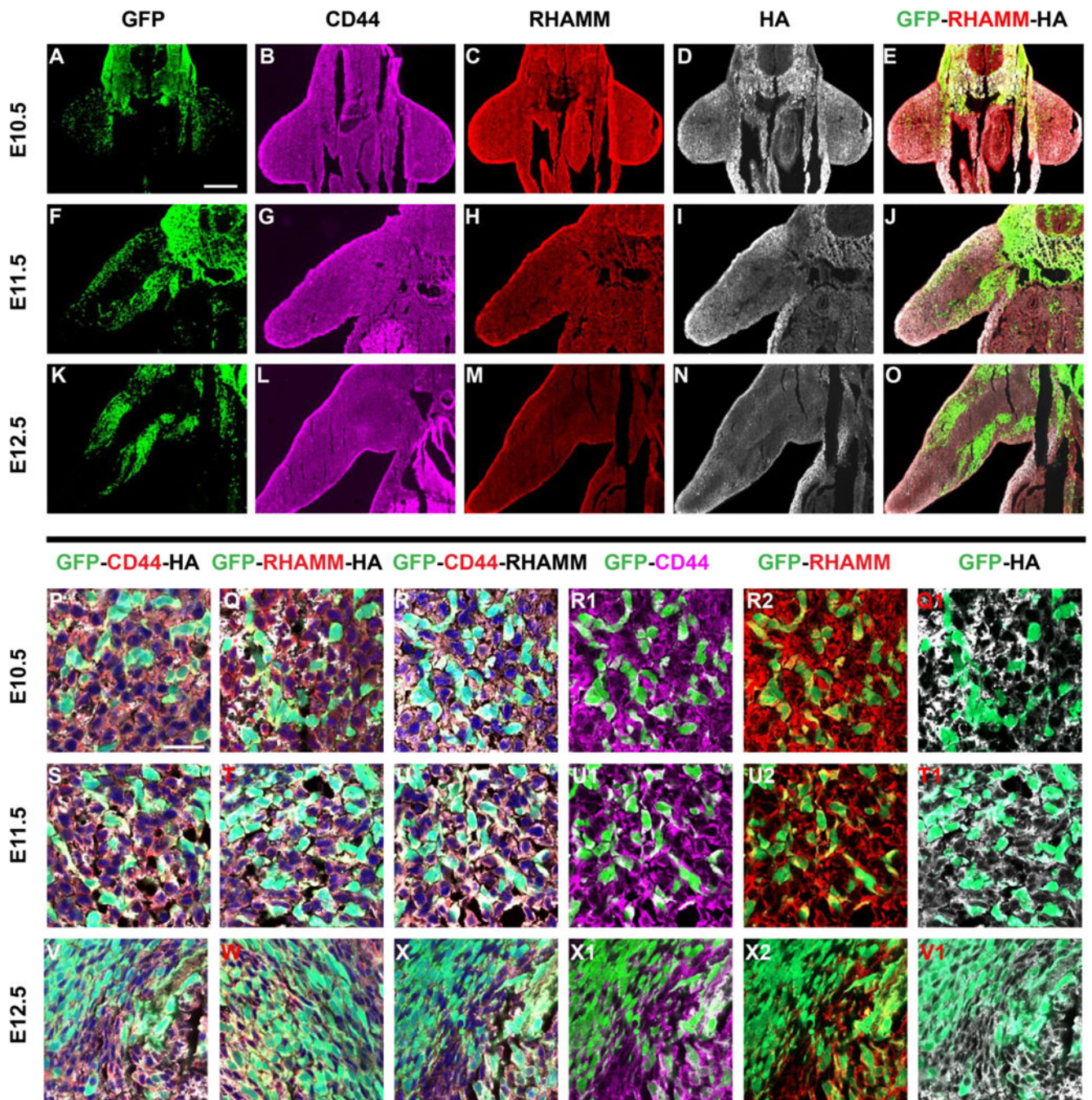


**Fig. 1.**

The overall distribution of CD44, RHAMM and HA in the developing forelimb from E10.5-E12.5.;(A-O) Serial sections of Pax3-Cre:ROSA-ZsGreen E10.5-E12.5 forelimbs were fluorescently labeled for CD44 (magenta), RHAMM (red) and HA (white). 5, $\times$  bar = 300 $\mu$ m. (P-X) Higher resolution images of E10.5-E12.5 forelimb muscles. 63 $\times$ , bar = 25 $\mu$ m.



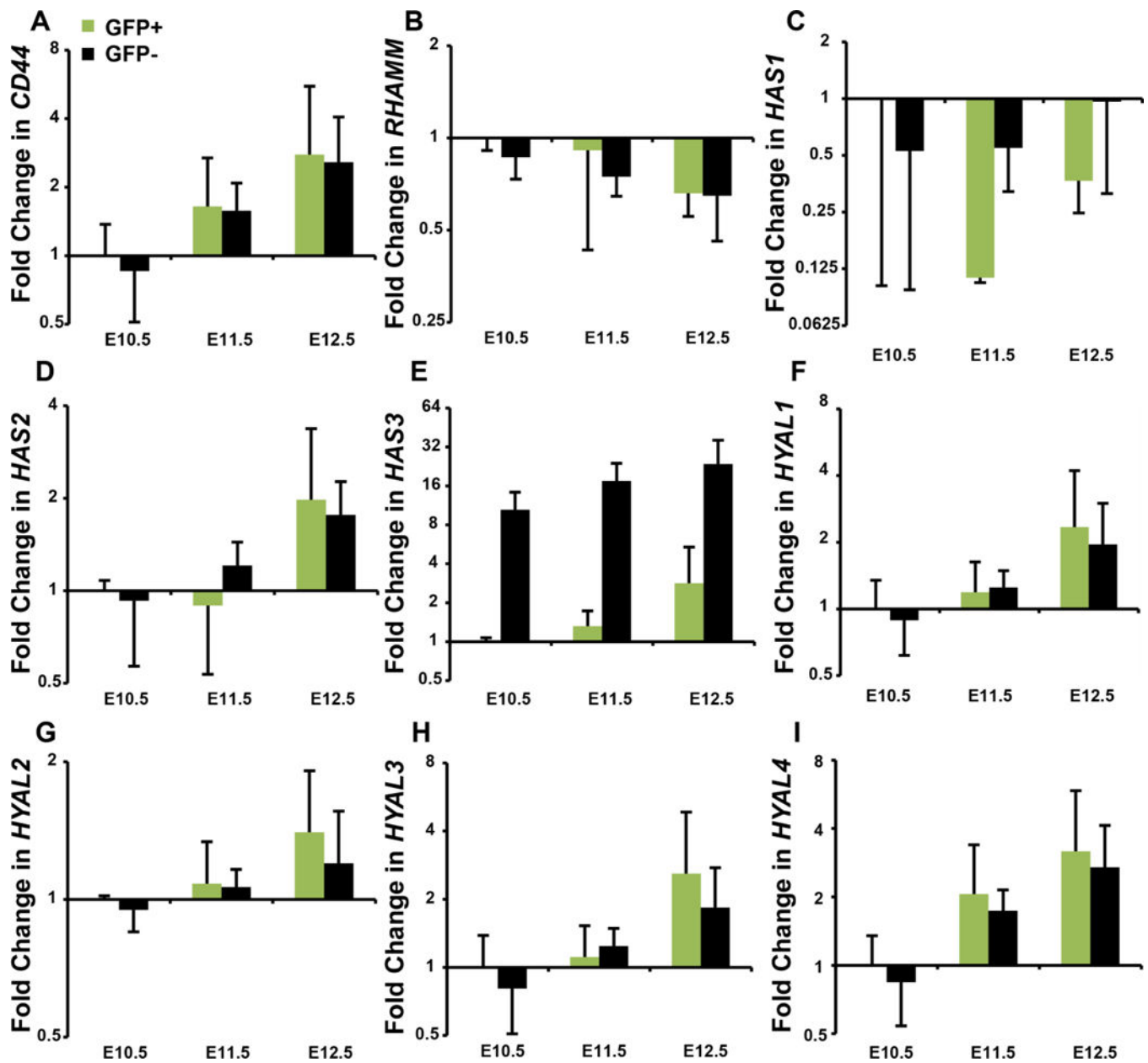


**Fig. 2.** Differential expression of HA-related genes during forelimb development. GFP+ and GFP- cells were isolated by FACS and gene expression was analyzed using qPCR. The fold change in different genes was calculated via the  $\Delta\Delta C_q$  method using B-actin as a housekeeping gene. To enable comparison between developmental stages, the expression of each gene was normalized to the fold change of E10.5 GFP+ cells. Log<sub>2</sub> scale; geometric mean of n = 3 biological replicates; error bars = S.D.

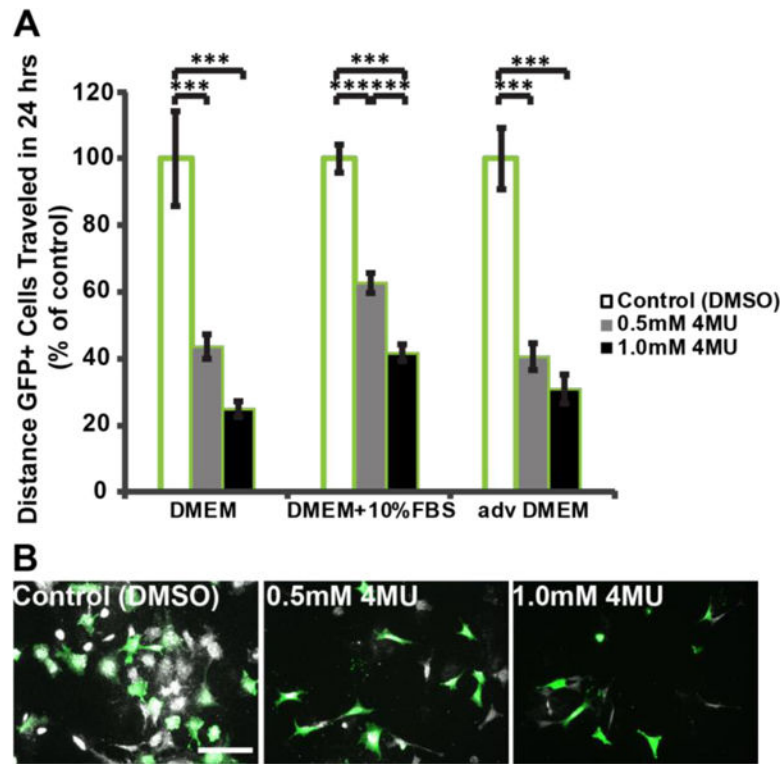


**Fig. 3.** 4MU treatment significantly inhibited GFP+ cell migration. A) Cells isolated from E10.5/E11.5 Pax3-Cre/ZsGreen forelimbs were tracked for 24 hrs. \*\*\* $p < 0.0001$ , error bars = S.E.;  $n = 55$  cells/condition across three biological replicates. B) Confirmation that the deposition of HA (white, HABP), in DMEM+10%FBS medium, was decreased by 4MU treatment. Green = GFP; bar = 100  $\mu$ m; 20 $\times$ .



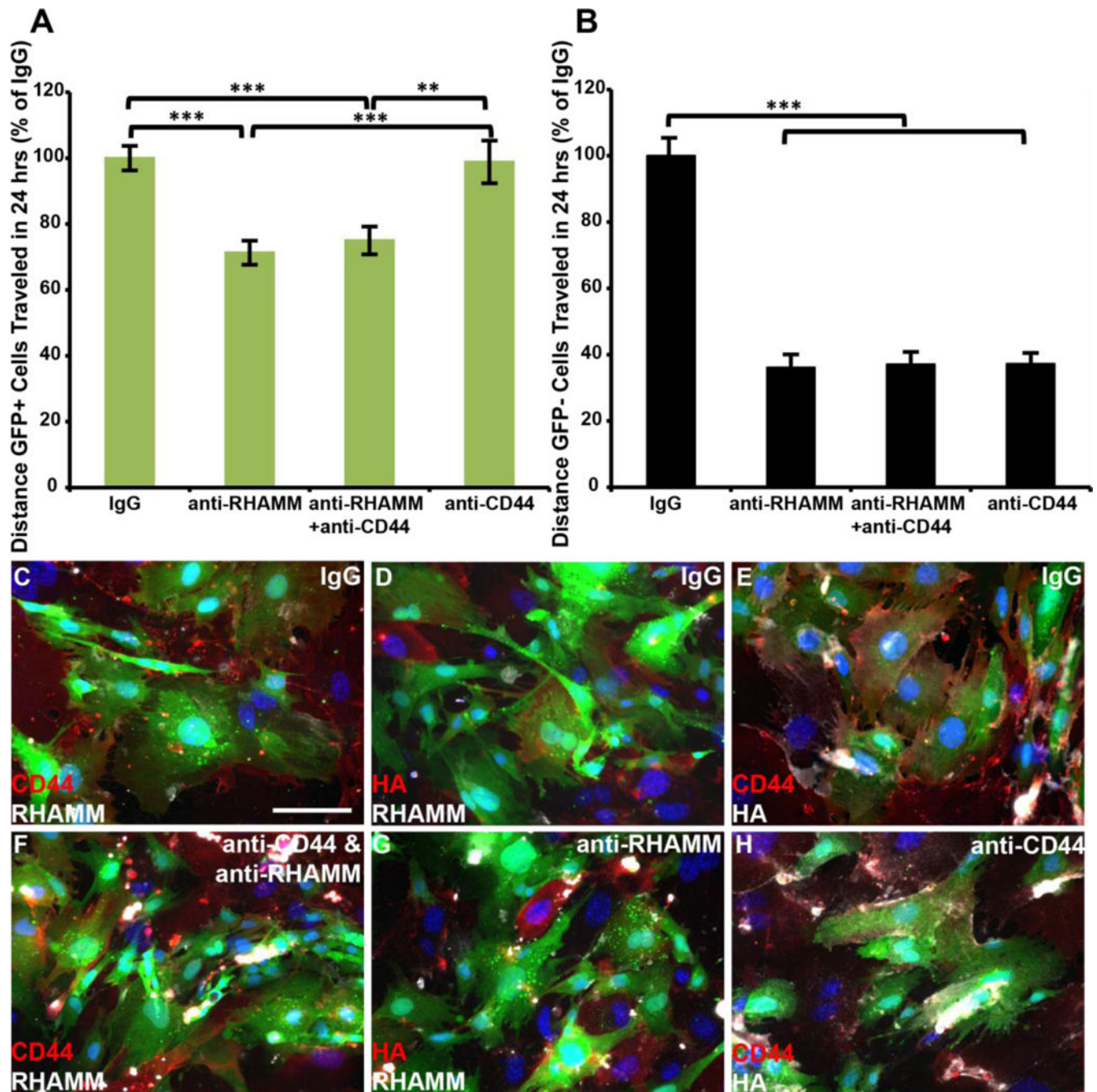


**Fig. 4.** The influence of CD44 and RHAMM on migration varies between cell types. A, B) anti-RHAMM significantly decreased the total distance GFP+ cells migrated over 24 hrs, whereas both antibodies inhibited the migration of GFP- cells. (\*\* $p < 0.0001$ , \*\* $p < 0.01$ ; error bars = S.E;  $n = 80$  GFP+ cells/condition and  $n = 47$  GFP- cells/condition across the 3 biological replicates). C-H) The expression of HA, CD44 and RHAMM in control and antibody-treated cultures was confirmed by immunofluorescence analysis. Blue = DAPI; green = GFP; bar = 100  $\mu$ m; 20 $\times$ .

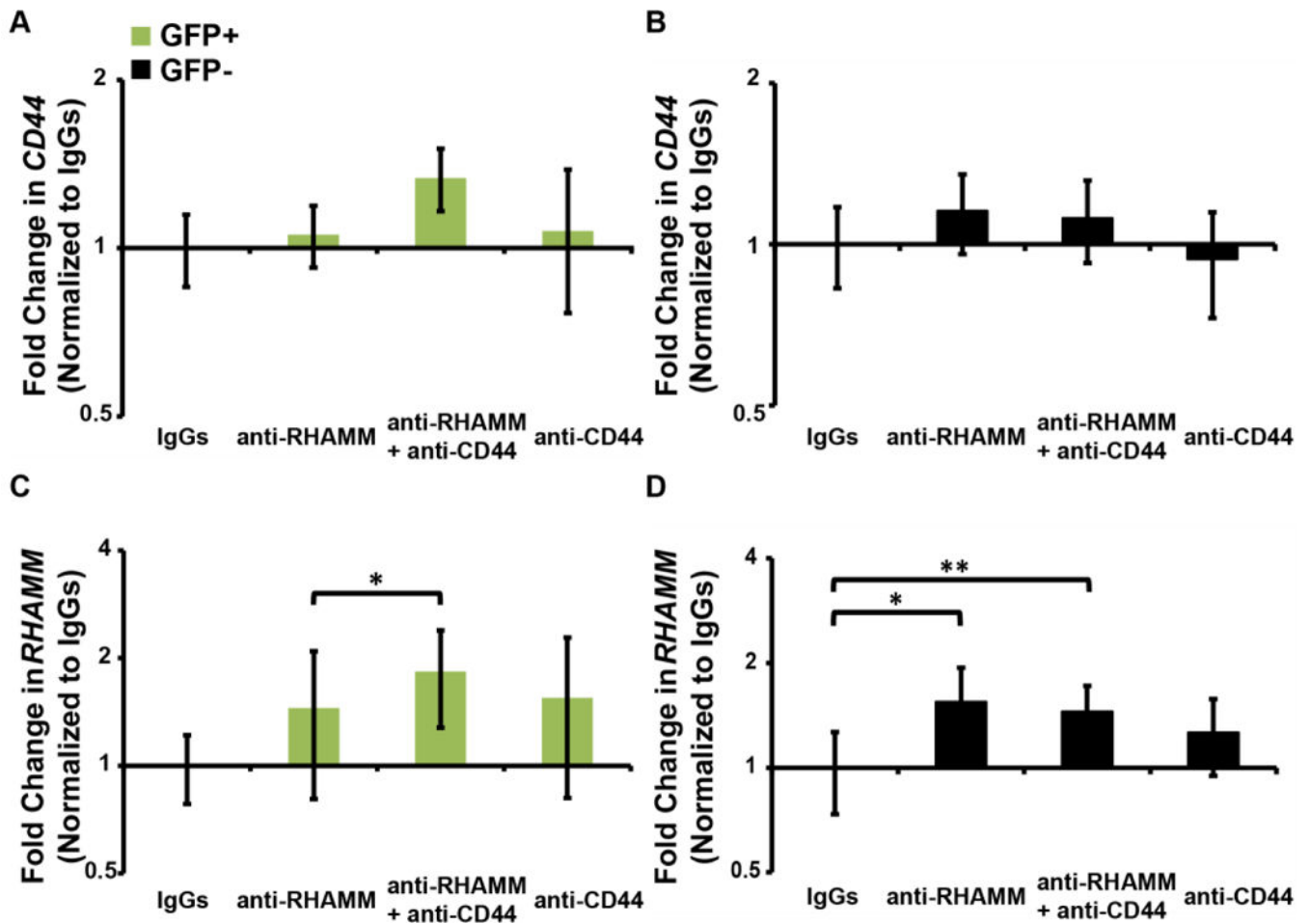


**Fig. 5.** Differential expression of HA related genes in GFP+ and GFP- cells after antibody treatment. Geometric means and standard deviation are plotted on a log<sub>2</sub> scale. One-way ANOVA followed by Tukey's post hoc test for assessing significant differences in fold changes between groups; \*p<0.05, \*\*p<0.01; error bars = S.D.; n = 3.

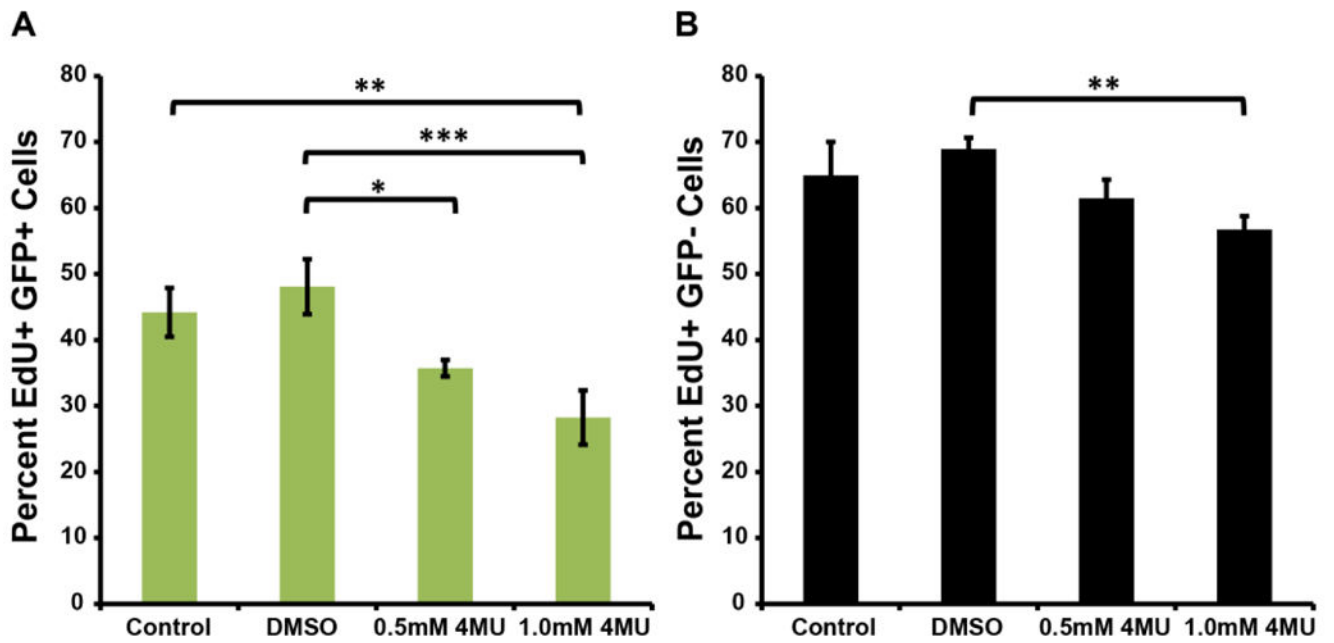


**Fig. 6.** 4MU significantly decreased cell cycle re-entry of embryonic forelimb cells. EdU incorporation by GFP+ and GFP- cells over 24 hrs was affected by 4MU in a dose-dependent manner. Two-way ANOVA followed by Tukey's post hoc test, \*\*\* $p < 0.001$ , \*\* $p < 0.01$ , \* $p < 0.05$ ; error bars = S.D.;  $n = 7200$  cells/condition across the 3 biological replicates and 3 technical replicates.

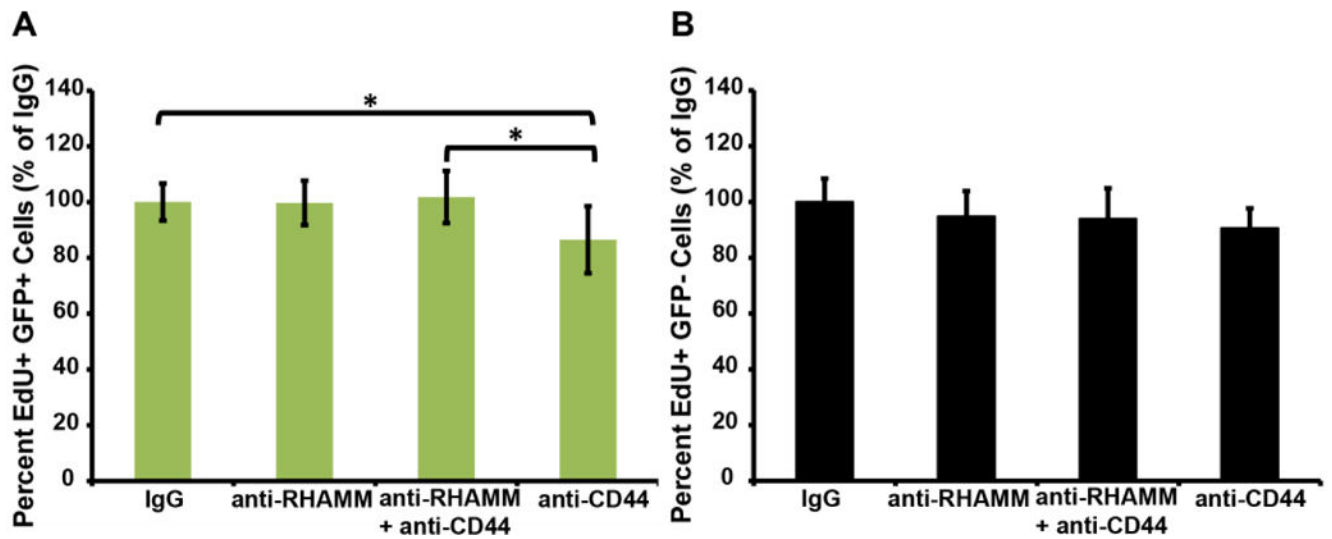


**Fig. 7.** Anti-CD44 but not anti-RHAMM significantly affected the proliferation of embryonic forelimb progenitors. GFP+ and GFP- cells, isolated via FACS, were labeled with 5  $\mu$ M EdU for 24 hrs while incubated with anti-CD44, anti-RHAMM or isotype controls. One-way ANOVA followed by Tukey's post hoc test, \* $p < 0.05$ ; error bars = S.D.;  $n = 8267$  GFP- cells and  $n = 13018$  GFP+ cells/condition across the 3 biological replicates.

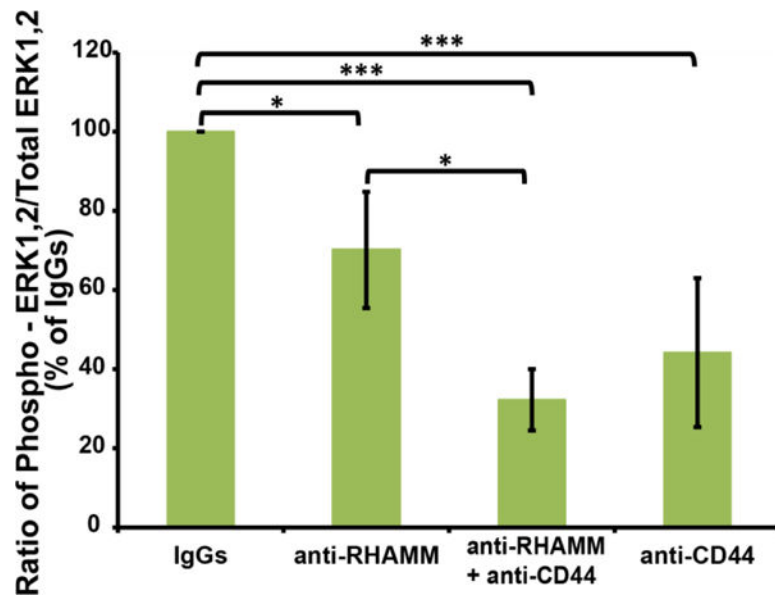


**Fig. 8.** Serum-induced ERK1,2 activation in GFP+ cells was inhibited by anti-CD44 treatment and anti- RHAMM. The ratio of phospho-ERK1,2/Total ERK1,2 was measured immediately before and after 30min serum stimulation. One-way ANOVA followed by Tukey's post hoc test across 3 biological replicates, \*p<0.05, \*\*\*p<0.001, error bars = S.D.

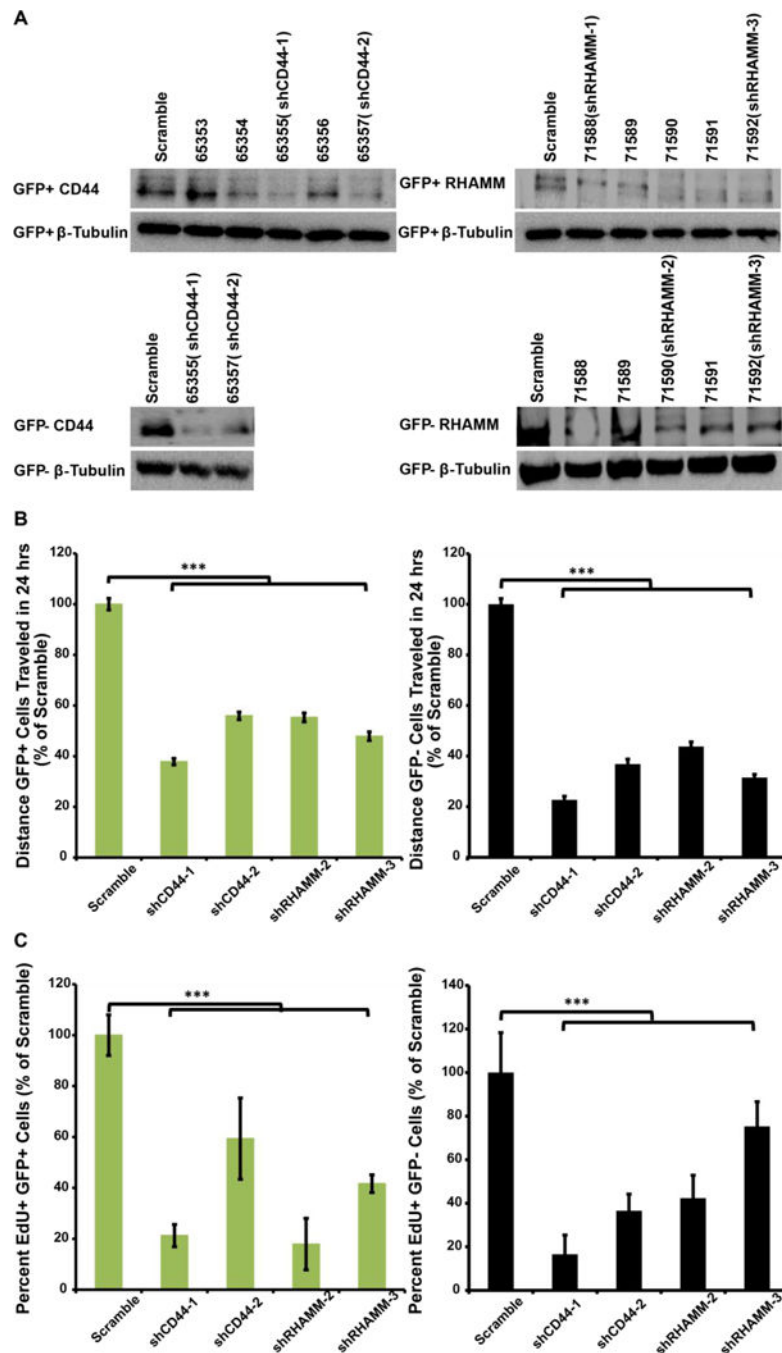


**Fig. 9.** CD44 and RHAMM depletion significantly affect both migration and proliferation of GFP+ and GFP- cells. A) Detection of CD44 or RHAMM depletion at protein level. Immunoblot analysis revealed reduction of CD44 and RHAMM protein using multiple shRNAs and the two most effective sequences were used for subsequent analysis. Detection of p-tubulin served as a loading control. B, C) Depletion of CD44 and RHAMM resulted in a significant reduction in the total cell migration (B) and proliferation (C) over 24 hrs. One-way ANOVA indicated shRNA treatment significantly affected migration and proliferation ( $p < 0.0001$ ).



Tukey's post hoc test was used to compare between samples for migration and proliferation assays (\*\*p<0.0001; For migration: error bars = S.E; n = 352 GFP+ cells/condition and n = 205 GFP- cells/condition across the 3 biological replicates. For proliferation, error bars = S.D.; n = 15164 GFP+ cells/condition and n = 9089 GFP- cells/condition across the 3 biological replicates).

Author Manuscript

Author Manuscript

Author Manuscript

Author Manuscript

**Table 1.**

Primers used for RT-PCR analyses of mRNA expression

Gene	Forward Primer 5'–3'	Reverse Primer 5'–3'	Size, bp	Ref Seq
CD44	ACCAAATGAAGTTGGCCCTGA	TCTTCTTCAGGAGGGGCTGAG	196	NM_009851.2
RHAMM	CCTTGCTTGCTTCGGCTAAAA	CTGCTGCATTGAGCTTTGCT	189	NM_013552.2
HAS1	GAGGCCTGGTACAACAAAAG	CTCAACCAACGAAGGAAGGAG	158	NM_008215.2
HAS2	GAGCACCAAGTTCTGCTTC	CTCTCCATACGGCGAGAGTC	154	NM_008216.3
HAS3	TGGACCCAGCCTGCACCATTG	CCCGCTCCACGTTGAAAGCCAT	156	NM_008217.4
Hyal1	TCATCGTGAACGTGACCAGT	GAGAGCCTCAGGATAACTTGGATG	98	NM_008317.4
Hyal2	GCAGGACTAGGTCCCATCATC	TTCCATGCTACCACAAAGGGT	116	NM_010489.2
Hyal3	TCTGTGGTATGGAATGTACCCT	TGCACACCAAATGGGCCTTA	53	NM_178020.3
Hyal4	ATGCAACTATTGCCTGAAGGAC	GGAAGTCGGCAGGTTT TAGG	122	NM_029848.1
Actb	CGACAACGGCTCCGGCATGT	CTAGGGCGGCCACGATGGA	87	NM_007393.3

CD44 and RHAMM primers were designed using Primer-BLAST (NIH). Other primers were taken from [11]